Reply to reviewer #1:

General comments:

In this study, the authors analyse the alongshore coastal current intraseasonal variability and associated hydrodynamic and biogeochemical changes at 12S off the coast of Peru using in-situ measurements acquired during the mars-July 2017 shipboard sampling program. The manuscript shows some interesting results. It allows documenting the alongshore circulation during the propagation of a downwelling CTW mode 1 using real observations. The results are in agreement with recent modelling studies carried out over a longer period of time. Also, they look at the effect of the intensified poleward flow on the coastal hydrological and biogeochemical ocean properties. The major weakness of the paper is that the authors can't extract the intraseasonal variations from the interannual/seasonal variations using the ship measurements making the interpretation of the results more difficult. I would advise the authors to provide a more throughout discussion of their results using remote sensed data (when possible). Also, having a model study will back up their hypothesis. Finally, one additional issue is that the manuscript is sloppily written (sometimes hard to get the sense), with clumsy wording and need proper editing. I will try to give some examples of this below. I will suggest to proof-read the manuscript by a native English speaker. Also, the figures are of good quality but the captions need to be reworked. Sentences in the captions are too long and some basics information are missing (full dates, units etc...). Overall, I find the manuscript worthy for publication in Ocean Science, after a major revision. Please find below a list of comments followed the flow of the text, that the authors should address in the revised manuscript.

We would like to thank reviewer #1 for his/her critical review of our manuscript as well as the corrections and suggestions to improve the manuscript. We believe to have significantly improved the revised version of the manuscript upon his/her remarks and suggestions.

As detailed below, major changes in the revised version include a detailed analysis of the wind forcing and sea level anomaly using satellite observations, a rewritten introduction, a more throughout discussion of the results and a better reasoning as far biogeochemical processes are concerned. We also corrected sloppy wording and figure captions.

In our detailed response below, comments by the reviewer are in bold letters and changes in the manuscript are expressed in italic letter.

Specific/technical comments:

1) In the Abstract, what is meant by less fixed nitrogen loss? I am not a biogeochemist and so I might misinterpret what is saying here but in reading this part

of the paper (and also the conclusion), I got the impression that the change in Nitrate was driven by changes in the rate biogeochemical processes. But, later on (in reading the results and the discussion), this does not appear to be the case?

Thank you for pointing this out. Indeed, the increase in nitrate is not due to changes in the rate of biogeochemical processes but due to the shortened residence time of the water masses in the Peruvian Upwelling System (PUS). The shortened residence time in turn is due to increased alongshore advection of the water masses within the Peru-Chile Undercurrent. We have reformulated the abstract and explain this in more detail later in the manuscript to be more clear about this result. The abstract now reads

An intensified poleward flow increases water mass advection from the equatorial current system to the study site. The impact of the elevated advection was mostly noticed in the nitrogen cycle. Shorter transit times between the equator and the coast off central Peru led to a strong increase in nitrate concentrations, less fixed nitrogen loss to N_2, and a decrease in the nitrogen deficit.

2) l21-22: The introduction could be better structured and clearer. As an example try to define Peru Upwelling System (PUS) at the beginning of your introduction.

Thank you. We now define the Peru Upwelling System at the beginning of the introduction. Additionally, we restructured the introduction at several places to improve its clarity. The introduction now starts as

The Peruvian Upwelling System (PUS) is one of the biologically most productive regions in the world's ocean resulting in economically important fish catches (e.g. Carr, 2002; Chavez et al., 2008). Located in the Eastern Tropical South Pacific (ETSP), the high surface productivity of the PUS is most pronounced within 100 km off the Peruvian coast between 4 and 16° S (Pennington et al., 2006).

3) l22: Fig1: Too many details. Simplify to highlight only the surface and subsurface current mentioned in the text.

Agreed, we removed from figure 1 currents not mentioned in the text.

4) l34, l52: Be careful when defining acronyms to put the initial letter of each word in Capital. Re-check all over the manuscript.

Thank you, we have changed the spelling of words when introducing acronyms according to the suggestions.

Located in the Eastern Tropical South Pacific (ETSP), the high surface productivity … (Note that this acronym is now defined in the first paragraph due to the restructuring of the introduction.)

5) l48, l65, l168: timescales (try to be consistent over the manuscript)

Thank you for pointing out the inconsistent spelling. We changed *time scales* to *timescales* throughout the manuscript.

6) l50-53: Explain more how local wind modulate the intraseasonal variability (upwelling intensity, local CTW..)

Thank you, we agree with your comment and added a paragraph to the introduction explaining how local wind variability leads to variability of the PCUC. We also added a detailed analysis of local and remote wind forcing to the manuscript as suggested in your later comments. In the introduction we now state:

Intraseasonal variability of the eastern boundary circulation is either forced locally by changes of the wind system above the PUS or forced remotely by variability of the wind system at the equator. Strengthening (weakening) of the local alongshore winds causes intensified (reduced) Ekman divergence close to the coast that accelerates (decelerates) the coastal surface jet (e.g. Philander and Yonn, 1982; Yoon and Philander, 1982; McCreary et al., 1987; Fennel et al., 2012). At the same time, Coastal Trapped Waves (CTWs) are excited propagating poleward to set up an alongshore pressure gradient balancing the accelerating (decelerating) alongshore flow (Yoon and Philander, 1982). Due to differences in vertical structure of the surface jet and the excited CTWs, the poleward flowing PCUC accelerates (decelerates). Likewise, variability of local wind stress curl forces variability of the poleward undercurrent through enhancing or reducing Sverdrup transport in the eastern boundary current regime (e.g. McCreary and Chao, 1985; Marchesiello et al., 2003; Junker et al., 2015; Klenz et al., 2018). Local wind-forced variability of eastern boundary poleward undercurrents has been reported from the Californian, Mauritanian and Benguela eastern boundary upwelling regions on time scales from intraseasonal to seasonal (e.g. Allen and Smith, 1981; Marchesiello et al., 2003; Junker et al., 2015; Klenz et al., 2018).

7) l52: Coastal Trapped Waves (CTW). Also, be consistent over the manuscript on the use of CTW or CTWs

Thank you. We are now consistent in using CTW/CTWs over the manuscript.

8) l54: The sentence is incorrect, rephrase.

Indeed. We have rephrased the sentence ("Wind events in the equatorial Pacific can generate equatorial Kelvin waves that propagate eastward ") to

Variability of zonal winds in the equatorial Pacific forces equatorial Kelvin waves that propagate eastward.

9) l55: Not reflected but transmitted. "Upon reaching the continental margin, part of the EKW bounces back along the equatorial waveguide into westward propagating equatorial Rossby waves, while part of incoming energy is transmitted poleward along the southwestern coast of South America as CTW".

Yes, thank you. We have changed the sentence to

Upon reaching the continental margin, part of their incoming energy is transmitted poleward along the southwestern coast of South America as CTWs.

We did not include the Rossby wave part, as their frequency range is limited and particular the energy of high frequency Kelvin waves (i.e. with periods from a week to a month) cannot bounce back into westward propagating equatorial Rossby waves.

10) l56: Poleward propagating CTW modulate the alongshore and vertical currents

Thank you, we extensively revised this part of the introduction. The first sentence of this paragraph now states

While modulating the alongshore circulation and vertical velocities, poleward propagating CTWs produce vertical displacements of the pycnocline of the order of tens of meters and sea level changes of a few centimeters (Leth and Middelton, 2006, Colas et al., 2008, Belmadani et al., 2012).

11) l59: The author should mention the influence of the CTW on SLA as sea level data are used in the Results' section to track CTW

Indeed, please see our reply to comment 10) above.

12) l60: this sentence is incorrect.

We agree. We altered this statement to be clear that local wind forcing and heat fluxes are the most important factors for intraseasonal SST variability and CTW contribution is of less importance.

On the other hand, intraseasonal sea surface temperature (SST) variability is suggested to be mainly driven by local winds and heat fluxes while CTWs play only a minor role (Dewitte et al., 2011; Illig et al., 2014).

13) l62/63: The influence of remotely-forced CTW

Changed

14) l63: an individual propagating CTW

Changed

15) l67: Rephrase

This part of the introduction was completely rewritten and this sentence is no longer in the text.

16) In the Data section, the description of the ERSSTv5 data used in Figure 1 is missing.

We have added a paragraph on the ERSST data to section 2.

Sea surface temperature from the NOAA Extended Reconstructed Sea Surface Temperature, Version 5 (ERSSTv5) dataset (Huang et al., 2017a) was used. This dataset provides monthly

values of SST on a 2°x2° grid based on in-situ temperature observations from several sources (Huang et al., 2017b).

17) l92- the investigation

Changed.

18) l168- were smoothed

Changed.

19) I will suggest to remove the position of the isopycnals from figure 2 and figure 3 as there are not useful for this section.

Indeed, the isopycnals do not contribute to the analysis of circulation variability in section 4.1. However, we find it helpful for comparing the velocity distributions with the hydrographic sections and nutrient distributions shown in figures 8 and 10. These figures depict the same isopycnal surfaces. Therefore, we decided to keep the isopycnals in the figures.

20) l209: Check the notation figure for Ocean Science: Fig. 2b and not Fig. 2(b)

Thank you for this comment. We have changed the notation throughout the manuscript.

21) l208 Sea surface height anomaly / SLA?

Indeed, we have changed *sea surface height anomaly* to *Sea Level Anomaly (SLA)* and consistently use the abbreviation throughout the manuscript.

22) l211: The author use cm.s-1 in the text. Change Figure to put the unit in cm.s-1 to be consistent.

Thank you for pointing this out. We have changed the units of velocity to m s^{-1} throughout the manuscript and are now consistent with the units presented in the figures.

23) l218: At these depths and offshore

Changed.

24) l225: data were

Changed as well.

25) l242: the meaning is unclear

Thank you. This section was greatly revised. We now discuss alongshore velocity differences between two periods instead of alongshore velocity itself (also see comment 29) below. The sentence in question referring to a possible superposition of equatorward flow due to the Chile-Peru Deep Coastal Current and the CTW velocity signal is thus obsolete and was removed from the manuscript.

26) l232: The alongshore current modal structure of the three first modes

Changed

27) l227: Need to add the values of the velocity of the climatological alongshore current (Chaigneau et al., 2013) in the text which are necessary for the demonstration of the intensification of the PCUC. Also similarly to Figure 6 and figure 8, I would suggest adding a third panel to figure 3 to show the difference between the two periods of the amplitude of the alongshore current.

Thank you for this suggestion. We added a third panel showing the difference in velocity between both time periods to figure 3. Also, we added a sentence on the climatological alongshore velocities from Chaigneau et al. (2013) to facilitate an evaluation of the observed flow intensification.

The intensified PCUC flow strongly exceeds climatological PCUC flow reported from this region. Mean alongshore flow at 12° S determined from vmADCP data sampled during 22 cruises show maximum PCUC core velocities of 0.1 – 0.15 m s^{-1} (Chaigneau et al., 2013), similar to the situation observed during April 18-25 and June 24 (Fig. 2b and g).

28) l233: And the phase speed? Are they consistent with the theoretical values obtained in Illig et al 2018a?

The phase speeds of the first two modes are consistent with the values obtained by Illig et al. (2018a). However, the phase speed of the third mode is slightly below the range of their reported values. In the text, we now state:

The obtained phase speeds are within the ranges reported by Illig et al. (2018a, their table 1) for the first two modes while the phase speed of the third mode is slightly lower than their results (0.82 ms^{-1} compared to 0.93±0.08 ms^{-1}). The velocity structure of the modes is very similar to their structure reported in their study at 16°S as well.

The structure of section 4. Results was greatly revised. The CTW modes and their phase speeds are now discussed in section 4.1.3 Modal structure of the intensified flow.

29) l236-237: Wouldn't it be more accurate to compare the CTW modal structures to the alongshore velocities anomaly (i.e the difference between the 2 periods chosen)?

Indeed, thank you for this comment. In the revised version, we compare the modal structures to the difference of alongshore velocity between the two time periods and interpret it accordingly. We have modified Fig. 5 accordingly and adapted the text in section 4.1.3 and in the discussion.

30) l255: remove the second "and"

Removed.

31) I257: How are the zonal equatorial and coastal alongshore wind anomalies? Here the authors could add the intraseasonal variations of the winds superimpose to Fig5 or in another figure.

We thank the reviewer for this comment. In the revised version, we are including a detailed analysis of local and equatorial wind stress and wind stress curl variability in the results section and include a discussion of the results in the section 5. Summary and discussion. We show that local wind stress and wind stress curl forcing cannot explain the intensification of the PCUC. However, CTWs excited by local wind stress and Sverdrup transport likely have contributed to enhancing poleward flow later in May. We now show that an elevated westerly wind burst at the equator during April 2017 is likely responsible for the generation of a Kelvin wave that reached the eastern boundary beginning of May 2017. Here, it transmitted parts of its energy to a CTW moving poleward along the continental margin of South America. We have added the following sections to the results:

4.2.1 Role of local wind stress
A potential local forcing mechanism of the intensified PCUC flow are anomalies of local wind stress curl. An increase in the magnitude of near-coastal negative wind stress curl leads to increased poleward flow along the eastern boundary through Sverdrup dynamics (e.g., Marchesiello et al., 2003). The adjustment of the circulation to changes in the wind stress curl at the eastern boundary is rather fast and occurs within a few days (Klenz et al., 2018). Wind stress curl along the Peruvian continental margin between 10° S and 14° S was negative throughout the observational period (Fig. 4), continuously forcing poleward flow. However, during the period of PCUC acceleration between end of April and mid-May, the magnitude of negative wind stress curl decreased (Fig. 4c, d, e, f). It can thus be ruled out that local wind stress curl forcing is responsible for the observed intensified PCUC. Nevertheless, elevated negative wind stress curl was observed from May 18 – 22, which may have contributed to maintaining a strong PCUC in late-May.
Variability of near-coastal alongshore wind stress excites CTWs which propagate poleward (e.g. Yoon and Philander, 1982) and thereby enhance or decrease poleward flow within the depth range of the PCUC. Model studies show that CTWs are excited near the equatorward edge of the region of wind variability (e.g. Fennel et al., 2012). In Mid-April through May 2017, alongshore wind stress between 5° S and 15° S was variable (Fig. 5). While moderate wind stress (0.03-0.06 N m^{-2}) prevailed from mid-April to May 3, it was weak during the first two weeks of May (Fig. 5d,e, g). However, during the later period the strong acceleration of the poleward flow occurred, requiring an intensification of alongshore wind stress. Thus, the initial acceleration of the PCUC during this period (Fig. 2d, e) cannot be related to local wind stress variability. Alongshore wind stress did significantly strengthen on May 15 and remained elevated for a period of about 5 days. This wind event was intense between 15° and 5° S, but did not occur north of 8° S. CTWs were likely excited in the region between 12° and 8° S that contributed to the elevated poleward velocities observed in the later phase between May 17 and 26 (Fig. 2f).

4.2.2 Equatorial winds and wave response.
A weakening of the trade winds at the equator by e.g. westerly wind events forces downwelling on the equator which in turn generates an eastward propagating equatorial Kelvin waves, which in turn may have transmitted parts of its energy to a CTW at the eastern boundary. Indeed,

several westerly wind anomalies occurred in the central and eastern equatorial Pacific during the first 6 month of 2017 (Fig. 6). A particularly elevated westerly wind anomaly between the date line and 120° W occurred during the first two weeks of April (Fig. 6a). At the same time, a positive SLA propagating along the equator appears to the east of the wind event at about 100° W (Fig. 6b).

32) l258: suggests

Changed.

33) Section 4.3 and 4.4: This section describes the cross-shore structure of the hydrographic and biogeochemical tracers to the PCUC intensification during the two selected period. The text is too detailed which make it heavy to read. I think the major problem with the writing overall is simply too many words. Please simply.

We have shortened and simplified the manuscript throughout these sections.

34) l264-265: You do not look at the processes in this study. Rephrase

Thank you for pointing this out. We have rephrased this sentence to

In the following we analyse the changes in hydrographic conditions co-occurring with the increase of alongshore flow.

35) l266-269: This is an example of sentences that could be shortened. Please rephrase

We significantly shortened this section and removed repeated and unnecessary information. Former lines 266-269 now read:

Lower near-surface conservative temperatures near the coast compared to offshore (Fig. 8a, b) indicated active upwelling during the observational program. While the upwelling signal was restricted to the upper 50 m, near-coastal water masses between 50 and 300m were significantly warmer compared to water masses offshore (8a).

36) l277: I will found clearer to put the description related to the oxygen in section 4.4 (Response of the biogeochemical conditions to the PCUC intensification)

We agree that oxygen concentration may also be classified as a biogeochemical parameter. However, in the manuscript we discuss oxygen distributions analogously to temperature and salinity while in section 4.4 (discussion of biogeochemical parameters) we describe nutrient distributions and related parameters. The later discussion does not require linking to the distribution of oxygen concentrations. For us, it thus seems more clear to keep the current subsection separation. However, to make clearer that section 4.4 is restricted to the nutrient biogeochemistry we rename it as *"4.4 Response of nutrient biogeochemistry to the PCUC intensification".*

37) l285: Not many readers are familiar with the water masses characteristics off Peru. Please remind the reader what are the characteristics of the ESSW water masses (ESSW: T < 17◦C and S > 35; Silva and Neshyba, 1979; Chaigneau et al., 2013) in the text. Also, the authors may want to add a (small) panel with the position of the observations on a wider T/S diagram, with the T/S characteristics of the main water masses illustrated?

Thank you, we have added the T and S characteristics of ESSW and ESPIW to the text, in both cases we have relied on the most recent classification by Grados et al. (2018).

ESSW originates from the equatorial current system. It is characterized by a linear relationship of temperature and salinity in the temperature range 8 – 14 °C and absolute salinity range 34.6 – 35.0 (e.g. Grados et al., 2018). Lower salinity Eastern South Pacific Intermediate Water (temperature range 12 – 14 °C, salinity 34.8 (Grados et al., 2018)), which is also situated in the depth range mentioned above was only observed in the hydrographic data from two offshore stations (Fig. 10a).

38) l267: dates on Figure 6 are wrong

Thank you. An erroneous date was actually inserted in former Figure 3 and 7. We corrected the dates in the figures throughout the manuscript.

39) l303: an increase of 5 ...

Changed.

40) l358: The authors are looking at the total current vertical structure, not the anomaly.

Indeed, thank you. In the revised version we now discuss velocity anomalies that are presented in Figure 3 as suggested by the reviewer. We now highlight our hypothesis that the increase of PCUC velocities in May relative to April was caused by a CTW.

… that occurred simultaneously to the increase of poleward flow at 12 °S.

41) l363: attributed to the second and third CTW modes. They found poleward velocities along the Peruvian.

Changed accordingly.

42) l369: Could you explain how scattering will change the CTW vertical structure.

Scattering of the wave at changing topography will transmit the energy into higher modes. We included a brief explanation in the discussion:

The local topography interacts with the passing CTW as well and such an interaction is neglected in the CTW mode solutions derived here. […] At changes in the topography parts of the wave energy can be transmitted into higher modes or upstream scattering (Wang, 1980; Wilkin and Chapman, 1990; Brunner et al., 2019).

43) l371: the first CTW mode

Changed.

44) l376: show

Changed.

45) l378: alongshore winds

Changed.

46) l383: the advection

Changed.

47) l387-389: Total temperature/salinity cross-shore section during two periods (the initial phase and the peak of the poleward flow) along with the differences between the two periods are shown in figures 6a-f. Figures show an increase in temperature and salinity along the continental shelf under 100m, which is in agreement with the stronger transport/advection of warmer and saltier ESSW, poleward. The surprise is that negative "anomalies (differences between the two periods)" in temperature (Fig.6c) and salinity (Fig. 6f) are found in surface. I agree with the authors, this might result from the interannual/seasonal variations that have not been filtered from the signal analysed. However, this part of the discussion could be further elaborated (see general comment above), by (for example) looking at the SST from the satellites data from which intraseasonal variations can be estimated.

We agree with the reviewer that our discussion of temperature and salinity changes in the surface layer is very rudimentary; however, the main focus of our study is the circulation variability and its effect on hydrography and biogeochemistry. Given that section 4.3 and 4.4 are already quite long and detailed, as pointed out by the reviewer, we do not want to extend the analysis and interpretation of the surface signals.

48) l411: Does N-loss means biogeochemical processes? Could the authors respecified which ones and clarify this sentence?

Yes, the N-loss is a biogeochemical process that occurs within the ocean when there is no oxygen available (see e.g. Kalvelage et al., 2013). Bacteria use the oxygen atoms from nitrate (NO_3) and nitrate (NO_2) "to respire" and thus convert nitrogen nutrients to N_2 gas while consuming organic matter (i.e. they reduce nitrate and nitrite). We have added a description of the individual anaerobic biogeochemical processes when discussing the nutrient distribution to make this more clear and state when first mentioning N-loss:

The increasing nitrogen deficit is caused by the microbially facilitated reduction of nitrate, nitrite and ammonium to N_2 gas which occurs in anoxic waters during the consumption of organic matter (e.g. Kalvelage et al., 2013).

49) l412: Why would you expect this? Is the increase of Nitrate (and then, the reduce nitrogen deficit) not related to the stronger transport poleward in the PUS of high nutrient ESSW as shown by Echevin et al., 2014? You may want to re-specified (or show?) the mean Nitrate characteristics and provide the mean alongshore gradient of Nitrate to support your demonstration.

Indeed, the increase of nitrate is due to the advection of water with higher concentrations, but this spatial gradient is set by the biogeochemical N-loss. We state this more clearly now in the manuscript. In the T-S diagram we see an increase of nitrate for unchanged T-S conditions in the ESSW range, therefore the properties of the ESSW itself have changed.

Along the ESSW pathway within the PCUC from the equator to 12° S, the nitrogen deficit increases while nitrate concentrations decrease (Silva et al., 2009; Zamora et al., 2012; Kalvelage et al., 2013). The increasing nitrogen deficit is caused by the microbially facilitated reduction of nitrate, nitrite and ammonium to N_2 gas which occurs in anoxic waters during the consumption of organic matter (e.g. Kalvelage et al., 2013). The resulting nitrogen deficit accumulates with time during the poleward advection.

50) l423-425: the meaning is unclear

We have changed the sentence to be clear.

However, the increase of nitrate (and the sum of inorganic nitrogen species) exceeds the phosphate decrease by a ratio higher than the nitrogen to phosphorus relation implied in equation 1, therefore the nitrate change is more important than the phosphate change for the nitrogen deficit reduction.

51) l432: It won't be the case if equatorial waters were less rich in nutrients than the PUS. The sign of the anomaly depends on the sign of current anomaly and the sign of the gradient of the tracer (temperature or biogeochemical variables).

Indeed this depends on the sign of tracer gradient. As seen in their supplementary material the study by Bachèlery et al. (2016) is done in a setting of poleward nitrate decrease as well, we have added a mention of this to the manuscript.

In a model study in the Atlantic Ocean, were nitrate decreases poleward as well, it was shown that the total effect of CTWs on nitrate concentrations varies regionally …

52) l436: due to

Changed.

53) l438: Do the authors see changes in the coastal ecosystem? I wonder if the nutrient input associated with the downwelling CTW and the change in the N-P ratio is associated with a phytoplankton bloom as describe in Echevin et al., 2014. Have the authors looked at satellites chlorophyll data?

Thank you for this comment. Satellite data suggest a continuous decrease of chlorophyll concentrations from April to June in agreement with the seasonal cycle. An increase, which may have been caused by the nutrient advection due to the CTW was not evident. However, the model results from Echevin et al. (2014) described the simultaneous propagations of several modes of which the fastest mode was associated with the SLA and the velocity signal while CTW modes responsible for productivity change were of higher order.

54) l442- suggests

Changed.

55) l447- Again, at least, the small differences observed in temperature, salinity and oxygen could simply be due to the fact that the seasonal and interannual variations cannot be removed from signal analysed. This statement is too strong for the conclusion.

Yes, thank you. We have weakened this statement to express that in principal, no change of properties due to advection is expected without the existence of a respective horizontal gradient of the property.

For parameters without strong horizontal gradients, an increase in PCUC flow does not cause pronounced changes in the advection. In this study this applies to the conservative properties temperature and salinity as well as for oxygen where alongshore gradients are weak (Zamora et al., 2012). For these parameters there are no large differences between both circulation phases that can be attributed clearly to the altered circulation. Yet concentrations of nutrients are influenced by shorter transit times, being less altered by biogeochemical cycling.

56) l449/451: I do not think that was shown here (or at least not pointed out effectively). This study does not show changes in the rate of N-loss but rather point out the stronger transport of nitrate as the mechanisms for the nitrate/nitrogen deficit anomaly (in line with the results of Echevin et al., 2014). To look at how the biogeochemical cycles are affected by the CTW propagation further analysis are required (for example the use of a model). I will rephrase this to make your point clearer.

We have changed the discussion to highlight our point that the amount of nitrate lost during the transport between the equator and 12 °S is lower for higher current velocities, because constant biogeochemical cycling rates cause less accumulated changes of concentrations during the shorter transit times.

57) l452: "On intraseasonal timescales": From April to May 2017, our results suggest an increase in nitrate due to the passage of an intraseasonal downwelling CTW...

We have changed the manuscript according to the suggestion.

For the period from April to May 2017, our study suggests an increase in nitrate levels due to the passage of an intraseasonal downwelling CTW. This contrasts with the decrease observed previously on interannual timescales caused by downwelling CTWs (Graco et al., 2017).

58) l453: A downwelling CTW?

We have added "downwelling" in the comparison to the study by Graco et al. (2017). See above in the answer to 57.

59) l454 outcomes

Changed.

60) l458: different from

Changed.

Reply to reviewer #2

General comments: This research presents the shipboard currents, hydrographic and biogeochemical properties observation and satellite remote sensed sea surface temperature and sea level anomaly over the slope off the central Peru-Chile coasts. The authors used these data to investigate the possible scheme that determines shift of the upwelling system associated with the eastern boundary current in the southern hemisphere. Their most striking conclusion is that the southward propagating coastally-trapped waves (CTW), sourced from the equatorial current, played key (the authors used the word "likely" in the abstract) roles in determining those aforementioned variability in the upwelling system, or these CTW strengthened the southward transport of the sub-surface waters, which then "supersedes the simultaneous effect of downwelling in terms of nutrient response". In my opinion, this conclusion is interesting, but still questionable, since the authors didn't provide sufficient solid analyses to support the schematic they drew in the abstract and conclusion section. Before presenting more specific comments, I have to admit that the results from their field measurements are invaluable and comprehensive, and the author put a lot of effort on the quality control and demonstrating them by using nice figures, although it took me some time to link the caption of those figures will the contents presented. Another great point of this research is that the authors did this research in a very interdisciplinary way. The combined discussion based on theories of physical and biogeochemical oceanography is very enlightening. The general comments, if I correctly summarized those specific ones, are that "the posted evidences cannot sufficiently support the conclusions" and "you need more evidences about the changes in the currents, not only in nutrient responses".

We would like to thank reviewer #2 for his/her encouraging but critical review of our manuscript and for the corrections and suggestions to improve the manuscript. We believe to have significantly improved the revised version of the manuscript upon his/her remarks and suggestions.

As detailed below, major changes in the revised version include a detailed analysis of the wind forcing and sea level anomaly using satellite observations, a rewritten introduction, an elaborate discussion of the possible impact of bathymetric features onto our alongshore flow observations, a more throughout discussion of the results and a better reasoning as far biogeochemical processes are concerned. Finally, we polished the writing of the text and the figure captions.

In our detailed response below, comments by the reviewer are in bold letters and changes in the manuscript are expressed in italic letter. We belief that some of the reviewer comments originated from sections where our writing was misleading. We hope to have corrected that in the revised version.

Specific Comments:

1) It is worthy for the authors to further polish their writing. The meaning of majority of those sentences is not easy to extract, since some sentences are too long and composed by many elements. I noticed that there is another published comment on the details about writing, and skipped them then.

We made great effort to improve the writing and comprehensibility of the manuscript. Please accept our apologies for not having done that before submitting the first version.

2) The authors listed too many details in the data processing section without paying sufficient attention to the interlinkages among these data. Yes, processing data is important, but it is more important for the authors to guide us towards the mainstream of their research flow by introducing the procedure of data processing. I can just get what did you do, this or that, but cannot understand why did you do that. There are too many subsections in the section 2. Please also make sure that tides are not important in determining the general characteristics of the general circulation in your study area.

Thank you for this comment. We significantly shortened the data and methods section wherever possible and tried to motivate our use of processing and analysis techniques. However, we think that our brief descriptions in the data and method sections are necessary to allow replicability of our results from the published data. The different subsections in section 2 and 3 will allow the reader to extract specific information on data or methods without needing to go through longer data or methods section. We thus decided to retain most subsections in section 2 and 3.

3) The introduction section is not well written either. The only points I can get are that the eastern boundary current and upwelling system experience multiscale variabilities that were not well studied, and the anomaly in winds (actually not only winds) can stimulate southward propagating CTW along the coastline. The authors didn't extract enough information from those cited historic studies to persuade us that CTW was found to greatly alter the regional upwelling processes, for example, strong downwelling signal from historic studies was observed during upwelling-favorable forcing conditions. Those historic studies were just cited in and out without sufficient investigation. The novelty of this research is missing in this section, although it is much better summarized in the summary section.

We agree with your comment. In the revised version, the introduction was reorganized and rewritten. We now focus on describing the Peruvian upwelling system, the consequences of variable nutrient and oxygen availability on biogeochemical processes, local and remote forcing of intraseasonal flow variability including effects of variable topography and the impact of intraseasonal flow variability on biogeochemistry. While doing so, we build upon historical studies. Finally, we improved the motivation of our study.

4) I don't quite understand why did the authors link the effect of CTW to the intraseasonal variability of eastern boundary current, especially when they didn't do any analyses on the wind (stress and its curl) fields in the manuscript. Although they compared the observed currents with the climatological ones from, for example, numerical simulations, we still don't know whether the wind is comparable to is climatological conditions during

the observation periods. Thereby, we cannot grantee that the variability is due to CTW, instead of migration of the wind system.

Thank you for pointing this out. We addressed this comment by including a detailed analysis of the wind variability prior and during the observed strengthening of the poleward boundary current flow. Additionally, we added a discussion of possible local wind forcing mechanisms in the introduction. Finally, we included an analysis of equatorial winds that triggered an equatorial Kelvin wave. In the results section of the manuscript, we added two subsections analyzing local and remote winds:

4.2.1 Role of local wind stress

A potential local forcing mechanism of the intensified PCUC flow are anomalies of local wind stress curl. An increase in the magnitude of near-coastal negative wind stress curl leads to increased poleward flow along the eastern boundary through Sverdrup dynamics (e.g., Marchesiello et al., 2003). The adjustment of the circulation to changes in the wind stress curl at the eastern boundary is rather fast and occurs within a few days (Klenz et al., 2018). Wind stress curl along the Peruvian continental margin between 10° S and 14° S was negative throughout the observational period (Fig. 4), continuously forcing poleward flow. However, during the period of PCUC acceleration between end of April and mid-May, the magnitude of negative wind stress curl decreased (Fig. 4c, d, e, f). It can thus be ruled out that local wind stress curl forcing is responsible for the observed intensified PCUC. Nevertheless, elevated negative wind stress curl was observed from May 18 – 22, which may have contributed to maintaining a strong PCUC in late-May.

Variability of near-coastal alongshore wind stress excites CTWs which propagate poleward (e.g. Yoon and Philander, 1982) and thereby enhance or decrease poleward flow within the depth range of the PCUC. Model studies show that CTWs are excited near the equatorward edge of the region of wind variability (e.g. Fennel et al., 2012). In Mid-April through May 2017, alongshore wind stress between 6°S and 15°S was variable (Fig. 5). While moderate wind stress (0.03-0.06 N m-2) prevailed from mid-April to May 3, it was weak during the first two weeks of May (Fig. 5d,e, g). However, during the later period the strong acceleration of the poleward flow occurred, requiring an intensification of alongshore wind stress. Thus, the initial acceleration of the PCUC during this period (Fig. 2d, e) cannot be related to local wind stress variability. Alongshore wind stress did significantly strengthen on May 15 and remained elevated for a period of about 5 days. This wind event was intense between 15° and 8° S, but did not occur north of 8° S. CTWs were likely excited in the region between 12° and 8° S that contributed to the elevated poleward velocities observed in the later phase between May 17 and 26 (Fig. 2f).

4.2.2 Equatorial winds and wave response.

A weakening of the trade winds at the equator by e.g. westerly wind events forces downwelling on the equator which in turn generates an eastward propagating equatorial Kelvin waves, which in turn may have transmitted parts of its energy to a CTW at the eastern boundary. Indeed, several westerly wind anomalies occurred in the central and eastern equatorial Pacific during the first 6 month of 2017 (Fig. 6). A particularly elevated westerly wind anomaly between the date line and 120° W occurred during the first two weeks of April (Fig. 7a). A positive SLA propagating along the equator appears to the east of the wind event at about 100° W (Fig. 7b).

Moreover, there were plenty of studies, for example, Zhang and Lentz [2017], have clearly showed that the response of shelf currents to the regional topography will also greatly modulate the domestic response of the current system. So, variability of the along-slope current itself is also worthy to be investigated.

We fully agree. However, as written above, the changes in local winds did not force the accelerated Peru-Chile Undercurrent. We added a discussion on the effect of variable bathymetry to section 6 (please also see our response to 5) below).

Talking about the time scale of intraseasonal, I also suggest the authors to investigate whether there are any meso-scale processes, for example, eddies, formed or detached from the main currents to generate the transition.

Our data set collected during the cruise as well as SLA data from satellites did not indicate any mesoscale eddy generation during the alongshore flow acceleration period. This argument also hold for the period of elevated flow from May 17 to May 26.

5) We knew that Kelvin waves or CTW will be continuously stimulated in its source region and propagate along the path you sketched. The authors used this process to explain the intraseasonal variability in the cold half year. Does that mean when the first CTW propagate through the system, the upwelling system will be shifted to a downwelling one and never switch back in the coming season? What will happen in, for example, December and January, when the downwelling system is switching back to an upwelling-dominant condition?

Thank you for pointing out difficulties in understanding our previous version of the manuscript. It was not our intention to argue that the described CTW is changing the state of the upwelling system. Instead, we use the term "downwelling CTW" exclusively to define the sign of velocity and SLA anomaly. In our definition, a downwelling CTW depresses the thermocline and is associated with an increase of SLA near the coast and enhanced poleward flow. However, as we also state in the manuscript, near-coastal surface temperatures decrease during the passing of the downwelling CTW. In more general terms, we cannot conclusively determine the impact of the CTW on the upwelling system itself. The decreased SSTs near the coast were not associated with enhanced but with declining chlorophyll concentrations. It is thus likely that elevated local wind from May 15 - 20 enhanced near-surface heat loss leading to cooling of the top few meters of the coastal water column. We added parts of this discussion to section 4.1 of the manuscript, where the near-surface cooling during the CTW event is mentioned.

The focus of our manuscript is on the variability of hydrography, oxygen and nutrient distributions in the upper thermocline of the Peruvian upwelling system. This depth range often lacks oxygen and variability of nutrients and oxygen here is very relevant for biogeochemical processes. We hope to have improved the focus of the paper by restructuring the introduction and by improving the discussion in the manuscript.

It was also known that those CTW will be domestically arrested by irregularity of the along-slope topography to form standing waves and alter the regional cross-slope processes. The recent study of Kämpf [2018] also showed that there will be downstream propagation of topographic waves after the strong current passing through an irregular

topography, for example, canyon or ridge. This is another possible process that determine the domestic response of the regional dynamics to the CTW or general disturbances in both barotrophic and baroclinic modes.

We thank the reviewer for pointing out that a discussion of the impact of irregular along-slope topography on the observed flow variability was missing in the previous version of the manuscript. In the revised version, we enlarged the insert in Fig.1 showing the distribution of topography between 10° S and 15° S and discuss topographic features near our sampling site. There is a small ridge to the north and the shelf narrows south of our sampling site. However, other than that there are no elevated topographic irregularities such as canyons. Nevertheless, CTW scattering at the upstream ridge can potentially increase the flow at our sampling site (Wang, 1980; Wilkin and Chapman, 1990). The narrowing of the shelf further downstream may also potentially influence the upstream circulation (e.g. as described by Wilkin and Chapman, 1990). However, we also point out that observations and models suggest that equatorially-forced first mode CTWs along the South American coast propagate past 25° S (e.g. Shaffer et al., 1997, Illig et al., 2018). As discussed by Illig et al (2018) in terms of the Burger number variability (Huthnance, 1978) the effect of stratification on the CTW parameters is found to be more important than irregular along-slope topography in the region of our sampling location. We added the following paragraph to the discussion in our manuscript:

Local bathymetry interacts with the passing CTW as well. North of our sampling site the continental slope bends offshore at depths between 500 m to 1000 m (Fig. 1, insert) and the shelf narrows south. Changes in coastline, shelf width, and along-slope bathymetry leads to a transfer of CTW energy into higher modes (scattering) and upstream backscattering (Wang, 1980; Wilkin and Chapman, 1990; Kämpf (2018); Brunner et al., 2019). The influence of the changes in shelf width on the upstream alongshore flow structure can extend to 200 km upstream (Wilkin and Chapman, 1990). Furthermore, the bent of the continental slope north of out sampling site may lead to CTW scattering which may additionally intensify the poleward flow at our sampling site. A recent model study suggests that differences between the theoretical CTW solutions and observations are predominately due to wave scattering (Brunner et al., 2019).

In summary, this study is a great try to advance our understandings on the transition of the eastern boundary currents, and they provided us invaluable observational evidences and detailed analyses. However, it is not easy for this single research (not their series of studies) to answer all those previous questions. I suggest the authors to investigate the spatial and temporal variation of winds (stress and curl) and variability of the currents from, for example, numerical simulations or some widely used global simulations (e.g. HYCOM and CMEMS) to expand the vision of this research and make sure that the variability is mostly determined by the southward propagating CTW, instead of the other processes, including, for example, migration of wind system, along-shore variability of slope current and response of slope currents to the domestic irregular topography. The authors didn't show us the general distribution of the regional topography, yet. The authors are also suggested to more explicitly define the timescale of intraseasonal variability in the manuscript. In my opinion, CTW may determine the synaptic variation of the current system, while migration of the wind system (and the associate variation in the

eastern boundary currents) will determine the entire background characteristics of the flow condition (upwelling or downwelling pattern). This will possibly be clearer than the term "intraseasonal" in your manuscript. A three-dimensional schematic of the flow pattern, propagation of CTW and responses in biogeochemical processes will greatly elevate this research, too.

We thank the reviewer for providing very valuable comments and suggestions for improving our manuscript. As detailed above, we considered most of his/her corrections and suggestions. We think that by including additional analysis of winds, sea level anomaly and irregular topography in the revised version of the manuscript, we provide sufficient evidence for understanding the nature of the observed flow intensification. Thus, we refrained from looking into global simulations such as HYCOM or CMEMS.

References: Kämpf, J. (2018), On the Dynamics of Canyon–Flow Interactions, Journal of Marine Science and Engineering, 6(4), 129.

Zhang, W., and S. J. Lentz (2017), Wind-driven circulation in a shelf valley. Part I: Mechanism of the asymmetrical response to along-shelf winds in opposite directions, Journal of Physical Oceanography, 47(12), 2927-2947.

Huthnance, J. M.: On Coastal Trapped Waves: Analysis and Numerical Calculation by Inverse Iteration, J. Phys. Oceanogr., 8(1), 74–92, doi:10.1175/1520-0485(1978)0082.0.CO;2, 1978.

Illig, S., Bachèlery, M.-L. and Cadier, E.: Subseasonal Coastal-Trapped Wave Propagations in the Southeastern Pacific and Atlantic Oceans: 2. Wave Characteristics and Connection With the Equatorial Variability, J. Geophys. Res. Oceans, 123(6), 3942–3961, doi:10.1029/2017JC013540, 2018.

Wang, D.-P.: Diffraction of Continental Shelf Waves by Irregular Alongshore Geometry, J. Phys. Oceanogr., 10(8), 1187–1199, doi:10.1175/1520-0485(1980)0102.0.CO;2, 1980.

Wilkin, J. L. and Chapman, D. C.: Scattering of Coastal-Trapped Waves by Irregularities in Coastline and Topography, J. Phys. Oceanogr., 20(3), 396–421, doi:10.1175/1520-0485(1990)0202.0.CO;2, 1990.

Influence of intraseasonal eastern boundary circulation variability on hydrography and biogeochemistry off Peru

Jan Lüdke[1], Marcus Dengler[1], Stefan Sommer[1], David Clemens[1], Sören Thomsen[2], Gerd Krahmann[1], Andrew W. Dale[1], Eric P. Achterberg[1,3], Martin Visbeck[1,3]

[1]GEOMAR Helmholtz Centre for Ocean Research Kiel, Düsternbrooker Weg 20, D-24105 Kiel, Germany

[2]LOCEAN-IPSL, IRD/CNRS/Sorbonnes Universites (UPMC)/MNHN, UMR 7159, Paris, France

[3]Kiel University, Kiel, Germany

Correspondence to: Jan Lüdke (jluedke@geomar.de)

Abstract. The Peruvian ~~Upwelling System~~upwelling system is characterized by high primary productivity fuelled by the supply of nutrients in a highly dynamic boundary circulation. The intraseasonal evolution of the physical and biogeochemical properties is analysed based on shipboard observations ~~and remote sensing~~ conducted between April and June 2017 off central Peru and remote sensing data. The poleward transport in the subsurface Peru Chile Undercurrent was highly variable and strongly intensified between mid and end of May. This intensification was likely caused by a first baroclinic mode ~~downwelling~~ coastal trapped wave excited at the equator at about 95° W that propagated poleward along the South American coast. ~~The~~An intensified poleward flow ~~shortens the time of~~increases water mass advection from the equatorial current system to the study site. The impact of the ~~anomalous~~elevated advection ~~is~~was mostly noticed in the nitrogen cycle ~~because during~~. Shorter transit times between the equator and ~~the shorter time needed for poleward advection less fixed nitrogen loss occurs within the waters. This causes~~coast off central Peru led to a strong increase ~~of~~in nitrate concentrations, less fixed nitrogen loss to N_2, and a decrease in the nitrogen deficit. ~~These changes suggest that~~The study highlights the importance of alongshore advection ~~caused by the~~due to coastal trapped ~~wave supersedes the simultaneous effect of anomalous downwelling in terms of~~waves for the nutrient ~~response.~~budget and the cumulative strength of N-cycling in the Peruvian OMZ.

1 Introduction

The Peruvian Upwelling System (PUS) is one of the biologically most productive regions in the world's ocean resulting in economically important fish catches (e.g. Carr, 2002; Chavez et al., 2008). Located in the Eastern Tropical South Pacific (ETSP), the high surface productivity of the PUS is most pronounced within 100 km of the Peruvian coast between 4° and 16° S (Pennington et al., 2006). Equatorward winds favour upwelling throughout the year (Bakun and Nelson, 1991; Strub et al., 1998) and enable a supply of nutrients from subsurface waters to the euphotic zone, stimulating high primary productivity (Pennington et al., 2006). Beneath the upwelling system, the low oxygen waters supplied to the PUS and enhanced local oxygen consumption due to remineralization of exported organic matter lead to the development of a pronounced Oxygen Minimum Zone (OMZ). The core of the OMZ with upper and lower bounds at about 30-200 m and 400-500 m depth, respectively, is considered to be fully anoxic (e.g. Ulloa et al., 2012, Thomsen et al. 2016).

The eastern boundary circulation ~~off Peru~~in the PUS is dominated by ~~wind driven upwelling near the surface and~~ the poleward Peru-Chile Undercurrent (PCUC) occupying the upper continental slope and shelf at depths ~~of about~~from 50 to 200 m (Fig. 1, e.g. Gunter, 1936; Chaigneau et al., 2013). It carries low-oxygen and high-nutrient Equatorial Subsurface Waters (ESSW), which constitutes the main source of the coastal upwelled waters (Brink et al., 1983; Penven et al., 2005; Silva et al., 2009; Albert et al., 2010; Chaigneau et al., 2013; Grados et al., 2018). Mean poleward velocities associated with the PCUC are

between 0.05 and 0.15 ms^{-1} (Chaigneau et al., 2013). The origin of its source waters is still under debate. Chaigneau et al. (2013) ~~back~~ traced its ~~origin~~source waters to the Equatorial Undercurrent supplying the PCUC via the Ecuador-Peru Coastal Current ~~flowing southward~~which flows poleward along the coast between the equator and 5 ~~°~~° S. In contrast, a regional model

40   analysis by Montes et al. (2010) suggests that the source waters of the PCUC originate predominately from the eastward Southern Subsurface Countercurrents south of the equator (Fig. 1). ~~Upwelling~~Above the PCUC, upwelling dynamics imply the existence of an equatorward geostrophic surface jet ~~above the PCUC,~~, known as the Peru Coastal Current (e.g. Hill et al~~.,~~., 1998; Kämpf and Chapman, 2016~~) as evidenced by model simulations (Montes et al., 2010). Additionally, observational and modelling studies suggest~~). Additional features of the eastern boundary circulation are the Peru-Chile Current flowing

45   equatorward ~~flow~~ offshore ~~(Peru Chile Current)~~of the PCUC and ~~below~~ (the Chile-Peru Deep Coastal Current~~)~~ flowing equatorward below the PCUC ~~as well~~ (Fig. 1, Strub et al., 1998; Penven et al., 2005; Czeschel et al., 2011; Chaigneau et al., 2013).

~~In the Peruvian Upwelling System (PUS) low oxygen, high nutrient Equatorial Subsurface Waters (ESSW) transported poleward by the PCUC upwells (Brink at al., 1983; Penven et al., 2005; Silva et al., 2009; Albert et al., 2010; Chaigneau et~~

50   ~~al., 2013; Grados et al., 2018). The PUS in the eastern tropical south Pacific (ETSP) is among the most productive regions in the world ocean resulting in economically important fish catches (e.g. Carr, 2002; Chavez et al., 2008). Equatorward winds favour upwelling throughout the entire year (Bakun and Nelson, 1991; Strub et al., 1998) and enable a supply of nutrients from the subsurface water to the euphotic zone feeding the high primary productivity (Pennington et al., 2006).~~

~~Beneath the upwelling system, the low oxygen waters supplied to the PUS and enhanced local oxygen consumption due to~~

55   ~~remineralization of exported organic matter lead to the development of a pronounced oxygen minimum zone (OMZ) and anoxic conditions between about 30-70 m and 400-500 m depth (e.g. Karstensen et al., 2008; Revsbech et al., 2009; Brandt et al., 2015; Thomsen at al. 2016). In anoxic waters, the microbial-mediated processes of denitrification and anammox convert bioavailable dissolved inorganic nitrogen (N), i.e. nitrate, nitrite and ammonium to nitrogen gas (N$_2$) and nitrous oxide (N$_2$O) which are subsequently outgassed to the atmosphere. N$_2$ fixation by diazotrophic organisms counteracts this loss of N-nutrients~~

60   ~~(N loss). It is still a matter of debate whether the global ocean N cycle is presently in balance (e.g. Gruber, 2004; DeVries et al., 2013). An imbalance of the N fluxes with more (less) N loss than N$_2$ fixation would reduce (enhance) future primary productivity and thus reduce (enhance) the capacity of phytoplankton to sequester CO$_2$ in the ocean (e.g. Codispoti, 2007).~~

The PUS exhibits variability on a wide range of ~~time scales~~timescales including intraseasonal (e.g. Brink et al., 1982; Gutiérrez et al., 2008; Belmadani et al., 2012; Pietri et al., 2014, Illig et al., 2018a, 2018b), seasonal (e.g. Pizarro et al., 2002; Chaigneau

65   et al., 2013), and interannual to decadal (Pizarro et al., 2002; Ramos et al., 2008; Graco et al., 2017). In particular, intraseasonal variability of oxygen and nutrient concentration along the Peruvian continental slope and on the shelf are known to strongly impact benthic and pelagic ecosystems within the OMZ and the upwelling region above (e.g. Gutiérrez et al., 2008; Echevin et al., 2014; Graco et al., 2017). A prominent benthic example is the biota responses to the frequency of oxygenation episodes changing from macro-invertebrates dominated biomass to bacterial mats (*Thioploca*) or when the frequency reduces (e.g.

70   Gutiérrez et al., 2008). Furthermore, the availability of nitrate nutrients in the anoxic waters of the OMZ allows for degradation of organic matter and is thereby consumed, while the lack of nitrate nutrients favours benthic sulfide emissions and sulfide plumes in the water column (e.g. Dale et al., 2016; Schunck et al., 2013). ~~). Intraseasonal variability is either forced locally by changes of the wind stress and its curl (e.g. McCreary and Chao, 1985; Klenz et al., 2019) or remotely with subsequent propagation of the variability in the form of coastal trapped waves (CTW) (e.g. Brink, 1982).~~

75   ~~Often, intraseasonal variability in the PUS is of equatorial origin and propagates poleward along the continental slope in the form of a CTW. Wind events in the equatorial Pacific can generate equatorial Kelvin waves that propagate eastward and upon reaching the continental margin are reflected into CTWs moving poleward along the shelf break (e.g. Enfield et al., 1987; Rydbeck at al., 2019). The poleward propagating CTWs modulate the velocities of the alongshore circulation (Shaffer et al., 1997; Pizarro et al.; 2002; Pietri et al., 2014), and thereby change the horizontal and vertical supply of nutrients. This affects~~

2

A key process thought to be responsible for the intraseasonal variability of the solute concentrations is variability of the eastern boundary circulation. Intraseasonal variability of the eastern boundary circulation is either forced locally by changes of the wind system above the PUS or forced remotely by variability of the wind system at the equator. Strengthening (weakening) of the local alongshore winds causes intensified (reduced) Ekman divergence close to the coast that accelerates (decelerates) the coastal surface jet (e.g. Philander and Yonn, 1982; Yoon and Philander, 1982; McCreary et al., 1987; Fennel et al., 2012). At the same time, Coastal Trapped Waves (CTWs) are excited propagating poleward to set up an alongshore pressure gradient balancing the accelerating (decelerating) alongshore flow (Yoon and Philander, 1982). Due to differences in vertical structure of the surface jet and the excited CTWs, the poleward flowing PCUC accelerates (decelerates). Likewise, variability of local wind stress curl forces variability of the poleward undercurrent through enhancing or reducing Sverdrup transport in the eastern boundary current regime (e.g. McCreary and Chao, 1985; Marchesiello et al., 2003; Junker et al., 2015; Klenz et al., 2018). Local wind-forced variability of eastern boundary poleward undercurrents have been reported from all eastern boundary upwelling regions on time scales from intraseasonal to seasonal (e.g. Allen and Smith, 1981; Marchesiello et al., 2003, Junker et al., 2015, Klenz et al., 2018).

Alternatively, intraseasonal variability of the eastern boundary circulation in the PUS may be of equatorial origin and manifested as a poleward-moving CTW as well. Variability of zonal winds in the equatorial Pacific forces equatorial Kelvin waves that propagate eastward. Upon reaching the continental margin, part of their incoming energy is transmitted poleward along the southwestern coast of South America as CTWs (e.g. Moore and Philander, 1977; Enfield et al., 1987; Rydbeck et al., 2019). Early measurement programs off Peru investigating intraseasonal alongshore current variability showed coherent CTW signals with periods of 5-50 days propagating poleward between 5° S and 15° S (Brink et al., 1980, 1983; Romea and Smith, 1983). Tide gauge data and the lack of correlated local winds suggested that the CTWs were predominately of equatorial origin. Similarly, intraseasonal CTW variability (50-day period) in the PCUC off Chile having velocity amplitudes of up to 0.7 m s^{-1} were shown to have originated from wind variability in the central equatorial Pacific (Shaffer et al., 1997). Modelling efforts confirm that equatorially forced intraseasonal CTWs propagate along the eastern South American coast to as far as 30° S (Hormazabal et al., 2002; Illig et al., 2018b).

While modulating the alongshore circulation and vertical velocities, poleward propagating CTWs produce vertical displacements of the pycnocline of the order of tens of meters and sea level changes of a few centimeters (Leth and Middelton, 2006; Colas et al., 2008; Belmadani et al., 2012). The combined effect alters the horizontal and vertical supply of nutrients in the PUS. Modelling efforts and satellite observations suggest that subsurface nutrient and chlorophyll intraseasonal variability in the PUS are mainly forced by remotely forced CTWs (Echevin et al., 2014). The simulations indicate that the shoaling and deepening of the nutricline, as well as the horizontal currents associated with the CTW induce a nutrient flux in and out of the euphotic layer, which impacts primary production. On the other hand, intraseasonal sea surface temperature (SST) variability is suggested to be mainly driven by local winds and heat fluxes while CTWs play only a minor role (Dewitte et al., 2011; Illig et al., 2014). On interannual timescales CTWs can dominate the variability in nutrient concentrations (Graco et al., 2017) and bottom water oxygen levels that can lead to strong changes in benthic ecosystems (Gutierrez et al., 2008).

Here, we use an extensive data set from a multi-cruise observational program to analyse the impact of an a strongly elevated individual CTW observed during several field campaigns in austral autumn 2017 off Peru near 12°S spanning propagating CTW on the circulation, hydrography and nutrient concentrations in the PUS. By visiting sampling stations several times over a period of more than two months. By repeating stations several times , we provide a time series that allows us to measured the

3

variability of the circulation and hydrographic and biogeochemical conditions almost continuously and can distinguish the intraseasonal variability from that ~~of~~on shorter time scales due to ~~local~~other processes. ~~The required high temporal resolution~~
~~is missing in long term time series data based on monthly or longer scales such as used by Graco et al. (2017) to analyse the~~
~~interannual variability. Previous studies of the intraseasonal variability are based on modelling (e.g. Echevin et al., 2014) or~~
~~restricted to circulation (e.g Pietri et al., 2014) or surface variables only (e.g. observations used by Dewitte et al. (2011) and~~
~~Illig et al. (2014)).~~

The conditions off Peru in early 2017 were further affected by anomalously warm temperatures in the upper ocean during
March associated with a coastal El Niño event (e.g. Garreaud, 2018; Echevin et al., 2018). Our observations on which this
analysis is based cover the declining phase of the coastal El Niño event in April and May when SST anomalies were decreasing.

2 Data

2.1 Ship data

Within the framework of the Collaborative Research Center 754 "Climate-biogeochemistry interactions in the tropical ocean~~"~~
~~R/V Meteor~~", we carried out a combined physical and biogeochemical sampling program in the ETSP ~~off Peru~~ from April to
June 2017 on R/V Meteor (Tab. 1). A regional focus during the ~~4~~four individual cruises of the sampling program was a transect
starting at shallow waters off Callao (Peru) at about 12 ~~°~~° S running offshore perpendicular to the coastline to water ~~depth~~depths
larger than 5000 m ~~more than~~ and >100 km offshore (Fig. 1). ~~In the following, this transect will be called the 12°S section.~~
During the first ~~cruise of~~ R/V Meteor ~~(Tab. 1)~~cruise M135, the 12 ~~°~~° S section was ~~occupied~~studied at the end of the cruise on
April 7 - 8. The two subsequent cruises M136 and M137 focused on benthic and pelagic work ~~along the 12 °S section. Time~~
~~consuming benthic~~off Peru between 11° and 14° S (Sommer et al., 2019, Dengler and Sommer, 2019). Benthic lander
measurements ~~(e.g. Sommer et al., 2016)~~ required the vessel to remain close to the ~~12 °S~~ section between April 18 and May
29, 2017, when repeated hydrographic and velocity measurements along the section were collected. The ~~12 °S~~ section was
again resampled during the final cruise M138 on June 24. In this study, we analyse shipboard velocity data ~~collected by ocean~~
~~surveyors~~, hydrographic profiles ~~from the repeat measurements at 12 °S~~ as well as oxygen and nutrient concentration
measurements ~~that were determined from water samples and optical sensors~~from the repeat measurements at 12° S.

2.1.1 Shipboard velocity observations

During the cruises upper ocean velocities were recorded continuously using ~~the~~two vessel-~~mounted ADCP~~Ocean Surveyor
Acoustic Doppler Current Profiler systems (vmADCP) ~~of~~installed on R/V Meteor. One ~~Ocean Surveyor~~ vmADCP was
operating ~~with~~at a frequency of 75 ~~kHZ~~kHz (OS75). ~~During different phases of~~System configuration during the cruises, ~~the~~
~~OS75 was recording velocity at~~ varied only in depth bin settings. Depth bins of 4, 8 or 16 m ~~depth,~~were chosen depending on
~~the availability of backscattering signals~~strength of the backscatter signal and the focus of the investigation. The second
vmADCP operated at 38 kHz (OS38) ~~and~~which recorded ~~32~~depth bins ~~covering a larger~~of 32m while sampling an increase
depth range ~~than~~(30-1000m) compared to the OS75 system. During post-processing, vmADCP velocities were corrected using
a mean amplitude and misalignment angle determined ~~by a~~from water-track calibration (e.g. Fischer et al., 2003).
Misalignment angles derived from individual ship accelerations and turns followed a Gaussian distribution having a standard
deviation of less than 0.65° for the OS75 and less than 0.75° for the OS38 (Sommer et al., 2019). A temporal trend was not
detectable. The ~~resulting error~~uncertainty of the ~~mean~~ misalignment angle calibration can be determined from its standard
deviation divided by the square root of the number of independent estimates (e.g. Fischer et al., 2003). For our data, more than
100 ~~stations is thus~~independent estimates were available for each cruise, resulting in an angle uncertainty of less than 0.1 ~~°~~.
~~An erroneous misalignment correction hinders the complete removal of the ship velocity from the observed velocities. Here,~~
~~the magnitude of the~~° and an associated velocity bias of ~~our data due to uncertainties in the alignment angle calibration is~~

4

~~below~~less than 1 cm s^{-1} for underway data. Fischer et al. (2003) ~~considered~~suggested an accuracy of 3 cm s^{-1} for ~~16 m bins in the upper 600 m under~~hourly underway data recorded during calm conditions in the tropics.

2.1.2 Hydrographic observations

At the 12 °S section a total of 151 hydrographic profiles were collected during the cruises M136 and M137 with a lowered SeaBird SBE 9-plus conductivity-temperature-depth (CTD) system using two pumped oxygen, temperature and conductivity sensors each. The CTD was attached to a General Oceanics rosette with 24 Niskin bottles of 10 l ~~each~~ to collect water samples. For the calibration of the conductivity sensor water samples were analysed with a Guildline Autosal Salinometer model 8400 B. ~~The salinity calibration was done using a linear fit with respect to temperature, pressure and conductivity of CTD measurements to the salinometer measurements. Oxygen calibration was performed using Winkler titration of water samples (Winkler, 1888; Grasshoff et al., 1983). Processing and calibration followed the GO-SHIP recommendations (Hood et al., 2010).~~ Correction coefficients for the CTD's conductivity sensors were derived using a multiparameter fit of the Autosal conductivities against the uncalibrated CTD sensor measurements. Coefficients included an offset and factors for temperature, pressure and conductivity.

CTD oxygen sensors were calibrated against oxygen concentrations determined from bottle water samples using Winkler titration (Winkler, 1888; Grasshoff et al., 1983). Processing and calibration followed the GO-SHIP recommendations (Hood et al., 2010). ~~From previous~~Previous studies using ~~STOX (~~Switchable Trace amount ~~Oxygen~~OXygen (STOX) sensors~~,~~ have shown that the core of the Peruvian OMZ ~~off Peru~~ is ~~known to be~~ anoxic ~~and in its core the oxygen concentrations are below the detection limit of the Winkler titration method~~ (Revsbech et al., 2009; Thomsen et al., 2016). ~~From all water samples collected within the supposedly~~Unfortunately, the Winkler titration method fails to accurately determine very low oxygen concentrations from bottle water samples. To assure anoxic ~~zone~~conditions in the OMZ core, a mean oxygen concentration offset ~~was calculated (~~of 2.26 µmol l^{-1}~~) and~~ was subtracted. ~~As we assume this offset to stem from oxygen entering the water sample during the sampling process, the subtracted offset was scaled by the relative apparent oxygen utilization (AOU). Calibration coefficients were derived using a multiparameter fit of corrected Winkler oxygen concentrations against uncalibrated CTD sensor measurements. Coefficients were derived for offset, pressure and pressure squared, temperature, oxygen and oxygen squared, as well as for the product of oxygen and pressure.~~

Calibration of the salinity and oxygen sensors was performed separately for each cruise, except for M136 where the mean of the calibration of the preceding and succeeding cruises M135 and M137 was used (M136 lacked the required deep-water samples). The final post-cruise calibration of the data resulted in an accuracy for temperature, salinity, and oxygen of 0.002 °C, 0.002 g kg^{-1} and 1.5 µmol kg^{-1}, respectively.

2.1.3 Nutrient measurements

Water samples collected ~~on~~during the upcast of the CTD rosette were used to determine nutrient concentrations. Concentrations of nitrate, nitrite and phosphate were measured using a QuAAtro autoanalyzer (Seal Analytical) with the precision of 0.1 µmol l^{-1}, 0.1 µmol l^{-1}, and 0.2 µmol l^{-1}, respectively (Sommer et al., 2019). Ammonium concentrations were measured using a fluorimetric ~~methodology according to~~method (Holmes et al. ~~(.,~~ 1999).

In addition ~~to analysed water samples~~, concentrations of nitrate were measured using a Satlantic Deep Submersible Ultraviolet Nitrate Analyzer (SUNA) mounted on the CTD rosette. SUNA measurements are based on the absorbance spectra of ultraviolet light (Sakamoto et al., 2009). Data post-processing followed Karstensen et al. (2017) and Thomsen et al. (2019). ~~Finally~~In a final step, the SUNA nitrate concentrations were calibrated against the nitrate ~~measurements by~~concentrations from the ~~autoanalyzer~~CTD water samples using a linear fit.

2.2 Additional data

~~In addition to the cruise data~~ To supplement our analysis of ship-board observations we used ~~sea level anomaly~~additional data sets. Sea Level Anomaly (SLA) data based on satellite altimeter measurements ~~that~~ were used – provided by the E.U. Copernicus Marine Environmental Monitoring Service (product: SEALEVEL_GLO_PHY_L4_REP_OBSERVATIONS_008_047). This is a level 4 dataset derived by merging all available satellite altimetry data into one gridded product. Reprocessed data from January 1, 1993 to January 1, 2018 with the release days January 15, 2018 (data before May 15, 2017) and May 16, 2018 was ~~used.~~accessed. Additionally, sea surface temperature from the NOAA Extended Reconstructed Sea Surface Temperature, Version 5 (ERSSTv5) dataset (Huang et al., 2017a) was analyzed. This dataset provides monthly values of SST on a 2°x2° grid based on in-situ temperature observations from several sources (Huang et al., 2017b). Finally, we analysed wind stress data from the ASCAT product of satellite scatterometer winds (Bentamy and Fillon, 2012). This product provides daily global winds and wind stress data with a resolution of 0.25°.

3 Methods

3.1 Analysis of velocity observations

The continuous velocity recording was split into segments when the ship was moving in on- or offshore directions only. The velocities were rotated to derive the alongshore component and then a mean velocity section was calculated for each segment of the cruise in 2 km bins according to offshore distance. Periods where the ship was moving slower than 1 kn were excluded~~, to restrict the analysis on periods where the ship was steaming.~~. To derive the sections of alongshore velocity over longer time periods, the data from several of these segments were averaged. The presented sections were smoothed using a 2D Gaussian weighting with an influence radius of 4 km (8 m) and a cut-off of 6 km (18 m) horizontally (vertically).

3.2 Analysis of hydrographic and biogeochemical data

The analysis of hydrographic data is based on the TEOS10 definitions (IOC et al~~.,~~. 2010) and conservative temperature, absolute salinity and (potential) density were calculated with the Matlab Gibbs Seawater Toolbox (McDougall and Barker, 2011; Version 3.05~~)~~). Nutrient concentrations were transformed to µmol kg^{-1} to remove the effect of compressibility on vertical gradients.

3.2.1 Nitrogen deficit

~~To analyse the importance of N-loss~~ In suboxic environments, microbially mediated biogeochemical processes ~~in waters off Peru during the advection~~such as denitrification and anaerobic ammonium oxidation (anammox) transform biologically available nitrogen nutrients (nitrate, nitrate and ammonium) into a form unusable by most organisms. These processes lead to ~~the 12 °S section, we determined the~~ a loss of nitrogen nutrients (N-loss) relative to other nutrients such as phosphorus. A metric for N-loss processes is the nitrogen deficit. A deficit (or excess) in nitrogen exists ~~if~~when the ratio of nitrogen to phosphorus deviates from ~~a~~the ratio ~~occurring during~~associated with the ~~assimilation~~synthesis and remineralisation of organic matter ~~(~~, i.e. the Redfield ratio~~), especially if N-loss or N$_2$ fixation is prevalent in the water mass~~ (Gruber and Sarmiento, 1997). ~~We apply an empirical formula~~Here, we used the formulation of ~~nitrogen deficit by~~ Chang et al. (2010) ~~which bases~~to investigate the nitrogen deficit. It is based on the deviation from the ratio between nitrogen species and phosphate ~~measured~~ outside of the eastern tropical south Pacific OMZ. The nitrogen deficit is calculated as:

$$N_{def} = 15.8 \, (PO_4^{3-} - 0.3) - (NO_3^- + NO_2^- + NH_4^+) \tag{1}$$

Where PO_4^{3-}, NO_3^-, NO_2^-, and NH_4^+ are the concentrations of phosphate, nitrate, nitrite and ammonium, respectively. With this definition, positive values of N_{def} quantify the N-loss that has occurred within a certain water mass while it has remained within the Peruvian OMZ.

3.2.2 Section averaging

Hydrographic and biogeochemical properties along the 12° S section analysed in this study have beenwere calculated by first interpolating the data onto common potential density surfaces. Performing the furthersubsequent analysis in density space removes the effect of internal waves which can cause strong up- or downward displacementselevated variability of vertical displacement of properties in the water column. The profiles have beenwere then averaged in bins of 2 km according to distance from the coastline in density space, this was done to include frequently sampled stations only once in the sections. Averaging over several profiles at the same station allows reducing the impact on the result of variability on shorter time scales than the averaging period.. The data waswere smoothed using a 2D Gaussian weighting with a density influence range (standard deviation of the Gaussian distribution) of 0.03 kg m^{-3} and a cut-off range of 0.05 kg m^{-3} and respectively an influence and cut-off range of 3 and 6 km within 40 km of the coast, 7 and 15 km within 80 kmfor the distances between 40 km and 80 km offshore and 15 and 20 km for more than 80 km offshore. The decreasing scale of horizontal interpolation towards the coast was used to benefit from the increased number of profiles to displaypreserve smaller scale features. Finally, the fields wereaveraged and interpolated onto the mean section of potential density calculated inproperties were transformed back into depth space.

3.3 Sea level anomaly and wind data

The SLA along the 12° S section was calculated by averaging all daily data points of gridded SLA data between 12° and 12.5 °° S over the time periods used for the velocity sections and interpolating them onto the section according to the distance to the coast. Grid points closer than 30 km to the coast have been excluded. The mean SLA along the section was subtracted in order to restrict it on the on-offshore gradient.to focus on the cross-shore gradient. Intraseasonal variability along the equator and coastline was analysed by subtracting the mean SLA over the 25-year time series before bandpass filtering SLA using a 4th order Butterworth filter for a time window between 20 and 90 days. To follow intraseasonal SLA variability due to propagating waves along the equator and subsequently along the western South American coast, we used bandpass filtered SLA data averaged between 0.25° S and 0.25° N from the equator and two-grid-points averages from near the coast.

To analyse intraseasonal variability along the equator and coastline at each grid point the mean SLA over the 25-year time series was subtracted before bandpass filtering using a 4th order Butterworth filter for a time window between 20 and 90 days. The wave track along the equator and the South American coast was calculated by averaging the bandpass filtered SLA between 0.25 °S and 0.25°N (equivalent to 2 grid points) along the equator and by averaging the two grid points closest to the coast for the coastal wave track.

For investigating wind forcing of Kelvin waves at the equator, SLA and zonal wind anomaly were averaged to five-day means over 10° of longitude. Additionally, wind anomaly was averaged between 5° N and 5° S while SLA was averaged between 2° N and 2° S.

3.4 Theoretical coastal trapped wave structure

To interpret the observed flow variability along the Peruvian coast in terms of CTWCTWs, the cross-shore-depth structure of CTWs was determined by considering the linear, hydrostatic, inviscid, and Boussinesq approximated equations of motion on an f-plane using local bathymetry and stratification (Brink, 1982; 1989; Illig et al., 2018a). For alongshore scales larger than cross-shore scales and horizontally uniform stratification, cross-shore-vertical mode structures (eigenfunctions) and

corresponding phase velocities (eigenvalues) solutions can be obtained from the simplified set of equations by using a resonance iteration approach (Brink, 1982; Brink and Chapman, 1987).

280 Here, we obtained the eigenfunctions and eigenvalues for the first three modes by applying a modified version of the Brink and Chapman (1987) Coastal-Trapped Wave programs as published by Brink (2018). These solutions have been used successfully in previous analyses of CTW structures in observational and model data (e.g. Brink et al., 1982; Pietri et al., 2014; Illig et al., 2018a).

Local bathymetry and stratification are required as input to Brink's (2018) set of Matlab mfiles. The ~~topography~~cross-shore
285 distribution of bathymetry was taken from the multi-beam echo sounder data collected during the cruises~~, a mean depth~~ along 12° S. Echo sounder data was ~~calculated~~averaged in 5 km bins ~~according to distance from the coast, resulting~~which resulted in a monotonic increase of water depth~~. Below~~ in offshore direction. Water depth lower than 5000 m ~~the depth was set to constant. The onshore closed boundary was set 10 km from the coast, effectively shifting the coordinate system, and with the depth measured 10 km off the coast.~~

290 were ignored. From two offshore CTD profiles (M136 #60 and M137 #92) exceeding 3000 m depth a stratification profile was calculated first for each profile using 20 data points with 1 dbar spacing and then a mean profile was calculated from both casts in 5 m intervals.

4 Results

4.1 Variability of the boundary circulation

295 ~~We observed the~~ Direct velocity observations from the multi-cruise program allow a detailed description of the variability of the eastern boundary alongshore ~~circulation~~velocity structure at ~~the~~ 12~~-°~~° S ~~section~~for a period of more than eleven weeks ~~by direct shipboard velocity measurements of the OS75 vmADCP~~ (Fig. 2). ~~From~~During the observational period from early April to June 24, 2017, ~~the eastern boundary circulation was highly variable. However, in the upper 100m and inshore of 40 km, flow was consistently~~ we captured an event of strongly increased poleward~~.~~
300 ~~In~~ flow that started in early May and lasted for about 35 days.

The time series started with two days of sampling in April~~, the~~ 7 to 8. During this period, a distinct poleward flowing PCUC was present that extended 80 km offshore (Fig. ~~2(a)) but then decreased in strength until~~ 2a) and had maximum velocities of more than 0.3 m s^{-1} on the continental shelf. Satellite altimetry indicated an increasing SLA towards the coast (Fig. 2a upper subpanel). Between April 18 and May 26 and except for a short break from May 4 to 6, the 12° S section was continuously
305 occupied. In mid-April ~~when~~poleward flow was present only on the shelf (Fig. ~~2(b)). The initially weak increase (1 cm over 40 km) of sea surface height anomaly towards the coast (Fig. 2(a)) vanished during this period as well (Fig. 2(b) and (c)). At the~~2b). However, from end of April~~, the PCUC started to increase in strength, extended further offshore and to greater depth. About 14 days later in~~ to mid-May, the PCUC ~~had strengthened~~ considerably ~~and its core reached~~strengthened reaching maximum core velocities of about ~~50 cm~~0.5 m s^{-1} between 50 and 100 m depth ~~-~~50 km offshore (Fig. ~~2(~~2c, d and e~~))~~~~). During~~
310 ~~this time period,~~). Furthermore, its poleward flow extended to more than 80 km offshore and it occupied the whole water column above 400 m depth. ~~Sea surface height anomaly~~The SLA increased towards the coast (by 2 cm over 40 km) implying that a poleward geostrophic velocity anomaly was present at the sea surface as well. ~~Towards the end of May,~~Towards the end of May, poleward flow in the PCUC did not increase further, but remained at a similar level as during mid-May (Fig 2f). In contrary, velocity data from a final section occupation 3 weeks later in June 24 evidence that the PCUC had weakened
315 drastically (Fig. 2g), exhibiting a comparable velocity distribution as between April 18-25 (Fig. 2b). Assuming similar time scales for its deceleration as for it acceleration, the period of intensified PCUC flow was between 30 to 40 days. The intensified PCUC flow strongly exceeds climatological PCUC flow reported from this region. Mean alongshore flow at 12° S determined from vmADCP data sampled during 22 cruises show maximum PCUC core velocities ~~slightly decreased but remained above~~

8

40 cm s⁻¹. No data are available from the first three weeks of June. However, during the final section occupation on of 0.1 –
0.15 m s⁻¹ (Chaigneau et al., 2013), similar to the situation observed during April 18-25 and June 24, the PCUC had weakened
drastically and maximum poleward velocities were only 10 cm s⁻¹ (Fig. 2((Fig. 2b and g))..

In April, the velocity sections indicated equatorward flow offshore and below the PCUC (Fig. 2). InAt these depth and offshore
ranges, the Peru Coastal Current and the Chile-Peru Deep Coastal Current are thought to be located (e.g. Penven et al., 2005).
When the PCUC weakened in; Chaigneau et al., 2013). In late April, the equatorward flow increased in strength and extended
to shallower depth (Fig. 2(b)2b and (c))..). However, during the period of strong poleward flow in May, the equatorward flow
decreased and was present only below 400 m depth close to the offshore end of the section (Fig. 2(e)2e and (f))..). On June 24,
weak equatorward flow was present below 200 m at most parts of the section but never reached velocities of 10 cm 0.1 m s⁻¹.
We found no indication of equatorward flow above or inshore of the PCUC, where the equatorward surface jet is expected to
be situated. The lack of this surface flow in observations was also previously noted by Chaigneau et al. (2013).

To compare the alongshore circulation with hydrographic and biogeochemical sampling, the data waswere averaged into two
periods: The initial phase of weak poleward flow (Fig. 3(a))3a) covering the period from April 18 – May 3, and a period of
elevated poleward flow 12-2926 May (Fig. 3(b)).

4.2 Coastal trapped wave characteristics

Coastal trapped waves are a known mechanism to intensify the 3b). The increase of poleward velocities is especially strong
between 40 and 60 km offshore where velocities increase from about zero to 0.4 m s⁻¹ (Fig. 3c). The core of velocity of the
alongshore increase is extending deeper than the intensified PCUC and is more detached from the coast.

4.2 Potential causes of circulation. To determine if variability

4.2.1 Role of local wind stress

A potential local forcing mechanism of the changes intensified PCUC flow are anomalies of local wind stress curl. An increase
in the magnitude of near-coastal negative wind stress curl leads to increased poleward flow along the eastern boundary through
Sverdrup dynamics (e.g., Marchesiello et al., 2003). The adjustment of the circulation to changes in the wind stress curl at the
eastern boundary is rather fast and occurs within a few days (Klenz et al., 2018). Wind stress curl along the Peruvian continental
margin between 10° S and 14° S was negative throughout the observational period (Fig. 4), continuously forcing poleward
flow. However, during the period of PCUC acceleration between end of April and mid-May, the magnitude of negative wind
stress curl decreased (Fig. 4c, d, e, f). It can thus be attributed to a CTW we compare ruled out that local wind stress curl
forcing is responsible for the observed velocity structure to the cross-shore intensified PCUC. Nevertheless, elevated negative
wind stress curl was observed from May 18 – 22, which may have contributed to maintaining a strong PCUC in late-May.
Variability of near-coastal alongshore wind stress excites CTWs which propagate poleward (e.g. Yoon and Philander, 1982)
and thereby enhance or decrease poleward flow within the depth structure of the range of the PCUC. Model studies show that
CTWs are excited near the equatorward edge of the region of wind variability (e.g. Fennel et al., 2012). In Mid-April through
May 2017, alongshore wind stress between 6°S and 15°S was variable (Fig. 5). While moderate wind stress (0.03-0.06 N m⁻²)
prevailed from mid-April to May 3, it was weak during the first 3 CTW modes (see section 3.4) and discuss SLA along the
coast for coherenttwo weeks of May (Fig. 5d, e, g). However, during the later period the strong acceleration of the poleward
flow occurred, requiring an intensification of alongshore wind stress. Thus, the initial acceleration of the PCUC during this
period (Fig. 2d, e) cannot be related to local wind stress variability. Alongshore wind stress did significantly strengthen on
May 15 and remained elevated for a period of about 5 days. This wind event was intense between 15° and 8° S, but did not
occur north of 8° S. CTWs were likely excited in the region between 12° and 8° S that contributed to the elevated poleward
velocities observed in the later phase between May 17 and 26 (Fig. 2f).

4.2.2 Equatorial winds and wave response.

A weakening of the trade winds at the equator by e.g. westerly wind events forces downwelling on the equator generates an eastward propagating equatorial Kelvin waves, which in turn may have transmitted parts of its energy to a CTW at the eastern boundary. Indeed, several westerly wind anomalies occurred in the central and eastern equatorial Pacific during the first 6 month of 2017 (Fig. 6). A particularly elevated westerly wind anomaly between the date line and 120° W occurred during the first two weeks of April (Fig. 7a). A positive SLA propagating along the equator appears to the east of the wind event at about 100° W (Fig. 7b).

This behaviour is similar to the appearance of the positive signals in the filtered SLA only east of 95° W (Fig. 6). A negative SLA anomaly occurs in the western equatorial Pacific at the time of the wave propagation and earlier (Fig. 7b) which may have been forced by the easterly wind anomaly at 160° E (Fig. 7a). But the SLA (Fig. 7b) reveals that the propagating negative SLA seen in filtered data (Fig. 6) does not occur throughout the basin and in the eastern Pacific the local minimum between phases of higher SLA is exaggerated by the filter. A downwelling CTW causes an increase of the PCUC, an increase of SLA and downward movement of subsurface isopycnal. The SLA and PCUC change suggest the existence of a wave of this sign. A first mode downwelling CTW would induce poleward transport across the upper 1500 m and we see poleward transport throughout the measurement range in the upper 1000 m. The existence of positive of a coherent high SLA along the eastern Equator and the South-American coast with poleward propagation does support the existence of a downwelling wave generated around 95° W as well, while the speed of the propagation suggests a first mode wave.

Similar to the velocity structure, SLA signals also support an association of the intensified poleward flow to the passage of a downwelling CTW. A downwelling CTW is associated with an upward elevation of the sea surface and a compensating downward displacement of the isopycnals in the water column as well as an intensification of poleward flow (e.g. Echevin et al., 2014). In this study we use the designation "downwelling" only to indicate the sign of velocity and SLA anomalies associated with the CTW. As discussed in the previous section, a local SLA increase was observed at the Peruvian coast while elevated poleward velocities within the PCUC depth range were present.

Bandpass-filtered SLA data from near the continental slope (section 3.3) indicates a positive SLA off Peru and Ecuador between the equator and about 14° S during this period (Fig. 6). The positive SLA along the coast propagates poleward at a velocity not inconsistent with a propagation speed of 3.1 ms^{-1}, the phase speed of the first CTW mode (Fig. 5). Moreover, when looking at SLA along the equator, there is a coherent signal starting at about 95° W moving towards the eastern boundary and arriving at about the same time when the SLA maximum of the coast is developing. Again, signal propagation from west to east is indicated, which agrees with the phased speed of a first vertical mode equatorial Kelvin waves (e.g. Yu and McPhaden, 1999). The SLA indicates the propagation of negative anomalies corresponding to an upwelling wave about 20 days earlier and with origin west of 140° W (Fig. 6) the arrival of this potential upwelling wave fits with the downward tilt in the SLA between April 25 and May 3 (Fig. 2c) and may contribute to the weak poleward flow by causing equatorward velocity anomalies.

4.1.3 Modal structure of the intensified flow

The cross-shore-depth structure of alongshore velocity obtained for the first three CTW modes at the 12° S section (see section 3.4) varies predominately in the vertical axis with poles of opposing velocity located above each other (Fig. 47). Flow reversal for each individual mode occurs at shallower depth away from the boundary compared to inshore regions. As expected, higher modes exhibit an upper pole of enhanced velocity at shallower depth compared to lower modes. and the phase speed (Fig. 7) decreases. The obtained phase speeds are within ranges reported by Illig et al. (2018a, their table 1) for the first two modes while the phase speed of the third mode is slightly lower (0.82 ms^{-1} compared to 0.93±0.08 ms^{-1}). The velocity structure of the modes is very similar to their structure reported in their study at 16° S as well.

For comparison, we show the difference of full-depth OS38 vmADCP alongshore velocities ~~averaged over the period of the strong PCUC in the upper ocean (~~between May 12 – ~~29,~~ 26 and April 18 – May 3 (Fig. ~~3(b)).~~7e). Apart from the ~~elevated~~increased poleward ~~velocities~~velocity in the upper 500 m, the alongshore velocity difference is weakly poleward throughout the upper 1000 m of the water column resolved by the OS38 (Fig. ~~4(e)).~~7e). When comparing the baroclinic structure of the observations to the baroclinic structure of the different CTW modes, it becomes obvious that due to the missing flow reversal ~~in our observations~~, the ~~observations are~~ observed change in alongshore velocity is best described by a first mode CTW. This mode features poleward flow anomalies throughout the upper 1500 m (Fig. ~~4(b)).~~7b) which agrees with the distribution of the velocity differences between the two time periods throughout most of the upper 1000 m (Fig. 7e). The maximum increase of ~~alongshore~~poleward flow, on the other hand, is ~~covering an area of the section better represented by~~ restricted to a depth range similar to the upper poleward velocity core of a second mode CTW ~~(Fig. 4(c)). However, it is possible that below the poleward flow of a first mode CTW, the equatorward Chile Peru Deep Coastal Current acts to reduce poleward velocities at depth between 500 m and 800 m.~~

~~Similar to the velocity structure, SLA signals also support an association of the intensified poleward flow to the passage of a downwelling CTW. As discussed in the previous section, a local SLA increase was observed at the Peruvian coast while elevated poleward velocities within the PCUC depth range were present.~~

~~Bandpass-filtered SLA data from near the continental slope (section 3.3) indicates a positive SLA off Peru and Ecuador between the equator and about 14°S during this period (Fig. 5). The positive SLA along the coast propagates poleward at a velocity not inconsistent with a propagation speed of 3.1 ms^{-1}, the phase speed of the first CTW mode (Fig. 4). Moreover, when looking at SLA along the equator, there is a coherent signal starting at about 95 °W moving eastwards to the eastern boundary and arriving at about the same time when the SLA maximum of the coast is developing. Again, signal propagation from west to east is indicated, which is in agreement with the phased speed of a first vertical mode equatorial Kelvin waves (e.g. Yu and McPhaden, 1999). The SLA indicates the propagation of negative anomalies corresponding to an upwelling wave about 20 days earlier and with and origin west of 140 °W (Fig. 5) the arrival of this potential upwelling wave fits with the downward tilt in the SLA between April 25 and May 3(Fig. 2(c)) and may contribute to the weak poleward flow by causing equatorward velocity anomalies.~~

~~A downwelling CTW would cause an increase of the PCUC and SLA suggest the existence of such a wave. A first mode downwelling CTW would induce poleward transport across the upper 1500 m and we see poleward transport throughout the measurement range in the upper 1000 m. The existence of positive of a coherent high SLA along the eastern Equator and the South American coast with poleward propagation does support the existence of a downwelling wave generated around 95 °W as well, while the speed of the propagation suggests a first mode wave.~~

4.3 Response of hydrographic conditions to the PCUC intensification

In the following we ~~will~~ analyse ~~if~~ the changes in ~~circulation affect the~~ hydrographic conditions ~~by changing~~co-occurring with the increase of alongshore ~~advection.~~

~~Upwelling causes a decline of SST towards~~flow. Lower near-surface conservative temperatures near the coast compared to offshore (Fig. 1~~) and the decline of surface temperature toward the coast was seen in conservative temperature along the 12 °S section as well (~~, Fig. 6(a) and (8a, b)~~)). However, the~~) indicated active upwelling during the observational program. While the upwelling signal was restricted to the upper 50 m, ~~deeper isotherms and isopycnals were bending downwards before intersecting the seafloor (Fig. 6(a) and (b)), not providing~~near-coastal water masses between 50 m and 300 m were significantly warmer compared to water masses offshore (Fig. 8a). During the intensified PCUC period (Fig. 8 middle panels) the cross-shore temperature gradient intensified, leading to an ~~isopycnal pathway towards the surface. The PCUC intensification co-occurred with a~~increased downward displacement of ~~the~~ isopycnals and isotherms ~~(Fig. 6(b)). This caused an increase in temperature in bottom waters below 50 m depth~~near the coast (Fig. ~~6(c)),~~8b). There, the ~~largest~~associated warming ~~of more~~

11

than 0.5 °C ~~occurred~~signal between ~~100~~100m and 200 m depth~~, on the other hand~~ was up to 0.5° C. It note that during the PCUC intensified period, near-coastal surface temperatures decreased ~~over the same time period~~.

Absolute salinity featured a shallow subsurface salinity maximum at about 25 m depth originating offshore and extending over the slope and shelf (Fig. ~~6(d)~~8d and ~~(e)). Below this~~(e)). As for temperature, cross-shore salinity ~~maximum the isohalines~~gradients were ~~bending downward towards the bottom. During~~evident between 50 and 300m depth with higher salinities near the coast which intensified when the PCUC ~~increase~~increased. At the~~ same time,~~ salinity ~~in bottom waters below 100 m increased but on~~at the upper shelf ~~in the top 100 m it~~ decreased (Fig. ~~6(f)).~~8f).

~~Dissolved~~Distribution of oxygen concentrations ~~off Peru~~were characterized by a sharp oxycline above the anoxic OMZ (Fig. ~~6(g)~~8g and ~~(h))~~.). During the ~~beginning of the measurement program from April 18 to May 3~~weak PCUC period, oxygen concentrations decreased from slightly supersaturated concentrations at the surface to anoxia within the upper 100 m of the water column (Fig. ~~6(g)~~8g). At depth between 450 and 500 m, oxygen concentrations started to increase again to detectable values (Fig. ~~6(g)~~8g). When the poleward flow intensified, low oxygen waters were found deeper in the water column following the downward displacement of the isopycnals (Fig. ~~6(h)~~8h). During this period, oxygen concentrations of 2 µmol kg^{-1} were found at 200 m depth in the bottom water (Fig. ~~6(h)~~8h), which has significant consequences for benthic and pelagic biogeochemical processes in that depth range discussed below.

In the upper water column above 400m, waters denser than 1025.9 kg m^{-3} were mainly Equatorial Subsurface Water (ESSW; Fig. ~~7). ESSW~~9). ESSW originates from the equatorial current system. It is characterized by a linear relationship of temperature and salinity ~~(cf.~~in the temperature range 8 – 14 °C and absolute salinity range 34.6 – 35.0 (e.g. Grados et al., 2018~~) and originates in the equatorial current system.~~). Lower salinity Eastern South Pacific Intermediate Water~~,~~ (temperature range 12 – 14 °C, salinity 34.8), which is also situated in the depth range mentioned above, was only ~~seen~~observed in the hydrographic data from two offshore stations (Fig. ~~7(a)).~~9a). The dominance of ESSW was not affected by the increasing poleward velocities (Fig. ~~7(b))~~9b) and most profiles follow the same temperature and salinity relationship in both phases. In fact, during PCUC intensification, the ESSW was the sole water mass in the upper 400m within 80 km of the coast (Fig. ~~7(b)).~~9b).

4.4 Response of ~~biogeochemical conditions~~nutrient biogeochemistry to the PCUC intensification

Nutrients are transported poleward by the PCUC and their advection thus is likely influenced by the variability of poleward velocity. In the following we describe the observed changes in nutrient concentrations and relate them to the variability in PCUC strength.

Nitrate concentrations on the shelf and upper slope increased when the poleward flow strengthened (Fig. ~~8(a)~~10a and ~~(b)).~~). The nitrate concentrations were low at the surface and increase with depth (Fig. 8 ~~(a)~~10a and ~~(b)).~~). During the initial phase, offshore surface nitrate concentrations decreased to less than 10 µmol kg^{-1} and ~~between the~~increased below to 20 µmol kg^{-1} at 50 m and 25 µmol kg^{-1} ~~isolines~~at ~~50 and~~ 300 m depth ~~patches of both higher and lower concentrations occur~~ (Fig. ~~8(a)).~~10a). Low concentrations in bottom waters on the shelf were most prominent between 75 and 100 m depth going down to 15 µmol kg^{-1} (Fig. ~~8(a)).~~10a). After the intensification of the PCUC, nitrate concentrations between 50 and 100 m depth offshore and 250 m in bottom waters increased ~~to above~~and exceed 25 µmol kg^{-1} (Fig. ~~8(b)).~~10b). Throughout this part of the section the increase exceeded 2.5 µmol kg^{-1} (Fig. ~~8(c)),~~10c), including areas with an increase in excess of 5 µmol kg^{-1} and even up to 10 µmol kg^{-1}. The surface layer featured ~~a nitrate increase~~anincrease in excess of 5 µmol kg^{-1} as well (Fig. ~~8(c)).~~10c).

Nitrite concentrations in the bottom water on the shelf and upper slope were reduced by the intensified PCUC (Fig. ~~8 (d)~~10d and ~~(e)).~~). The nitrite concentrations were low outside of the OMZ and their structure featured two maxima, the main one located in the centre of the OMZ around 300 m depth ~~reaching concentrations of 5 µmol kg^{-1}~~and the secondary maximum in the upper part of the OMZ at 150 to 200 m depth. After the intensification of the PCUC the upper boundary of nitrite containing water was displaced downwards, leaving bottom waters above 250 m depth free of nitrite (Fig. ~~8 (e)).~~10e). The depletion of nitrite in the bottom water was coupled to ~~the downward propagation of weakly ventilated water~~a weak ventilation supplying

485 oxygen (Fig. ~~6(h)).~~8h). This caused a nitrite decrease exceeding 2 µmol kg^{-1} in the bottom water around 200 m depth (Fig. ~~8(f)).~~10f).

Ammonium concentrations were generally low or undetectable. Concentrations in excess of 0.4 µmol kg^{-1} occurred only on the upper shelf and close to the surface (Fig. ~~8(g)~~10g and ~~(h)).~~), and were indicative of remineralisation of phytoplankton detritus, with rapid removal over time of the ammonium due to phytoplankton uptake and nitrification. ~~During the flow~~
490 ~~intensification the ammonium concentrations in the surface layer were reduced to less than 0.4 µmol kg^{-1} (Fig. 8(h)).~~ The patchiness of ammonium concentrations caused high positive and negative differences very close to each other on the shelf (Fig. ~~8(i)).~~10i). In the surface layer above 50 to 80 m in offshore waters, a decline of ammonium concentrations was observed. Phosphate concentrations did not change strongly by the increased strength of the PCUC (Fig. ~~8(j)~~10j and ~~(k)).~~). Concentrations were low at the surface and increased to 2 µmol kg^{-1} at 50 m depth. Within the upper OMZ the concentrations were higher
495 offshore than onshore (Fig. ~~8(j)~~10j and ~~(k)).~~). When the PCUC intensified, concentrations decreased below 50 m depth and above 100 m at 80 km offshore and 300 m inshore (Fig. ~~8(l)).~~10l). A phosphate decrease of up to 0.3 µmol kg^{-1} occurred in bottom waters on the shelf at water depths shallower than 100 m.

The nitrogen deficit was reduced in the later phase of the strong PCUC (Fig. ~~8(m)~~10m and ~~(n)).~~). During the weak PCUC phase the offshore maximum deficit was located between 150 and 200 m depth exceeding 12.5 µmol kg^{-1} and the absolute
500 maximum was a localized peak exceeding 15 µmol kg^{-1} in bottom waters just above 100 m depth (Fig. ~~8(m)).~~10m). This maximum on the shelf was caused by low nitrate (Fig. ~~8(a)~~10a and high phosphate concentrations (Fig. ~~8(j)),~~10j), while nitrite (Fig. ~~8(d))~~10d) and ammonium (Fig. ~~8(g)~~10g were enhanced as well. After the PCUC intensification the deficit reached 5 µmol kg^{-1} at about 70 m depth offshore and ~~at larger depths towards the coast, intersecting the seafloor at~~ 200 m depth at the coast (Fig. ~~8(n)).~~10n). At greater depths the maximum deficit exceeding 12.5 µmol kg^{-1} was located offshore around 150 m
505 depth, extending towards the coast along isopycnal surfaces. After the PCUC intensification, the nitrogen deficit in the upper 200 m inshore of 70 km was reduced (Fig. ~~8(o)).~~10o). The maximum decrease of the deficit occurred in the bottom water just above 100 m depth exceeding 10 µmol kg^{-1}; here the maximum described above in Figure 7(m) disappeared with the PCUC intensification. Further offshore around 100 m depth the decrease of the deficits exceeded 5 µmol kg^{-1} in several patches as well (Fig. ~~8(o)).~~10o).

510 The decrease in nitrogen deficit between 50 m depth and about 200 m depth (deeper toward the coast, and shallow offshore) exceeding 5 µmol kg^{-1} in its maximum agreed with the location of largest poleward flow (Fig. ~~3(b)).~~3b). At this vertical and horizontal range nitrate was increasing by more than 2.5 µmol kg^{-1} (Fig. ~~8(c~~10c) and phosphate decreased (Fig. ~~8(l)),~~10l), both changes contributed to the reduced nitrogen deficit. Nitrite concentrations decreased as well (Fig. ~~8(f)),~~10f), but the total increase in nitrogen species still exceeded the phosphate decrease by more than the ratio implied in equation (1), with the
515 nitrate change, dominating the change of nitrogen species.

The increase in nitrate concentrations and the decrease of the nitrogen deficit and phosphate concentrations are strongest in the upper 200 m where the intensified PCUC had its maximum during the same time period. These changes occurred when comparing both regimes in density space as well (not shown) and a nitrate increase within the ESSW was evident This suggests that poleward advection in the intensified PCUC is the main cause for the changes in biogeochemical properties while changes
520 due to vertical displacement only play a minor role, here.

5 Summary and Discussion

Measurements from an intensive physical and biogeochemical shipboard sampling program off Peru at 12 ~~°°~~ S are used to analyse intraseasonal variability of the eastern boundary circulation and associated changes in hydrography and nutrient distributions. The most prominent finding is an intensification of poleward velocities within the depth range occupied by the
525 PCUC that occurred throughout the last 3 weeks of May in 2017. During this period, maximum poleward velocities in the

PCUC core between 50 m and 100 m depth were above ~~50 cm s⁻¹ and the~~0.5 m s⁻¹ exceeding the reported mean state by far (e.g. Chaigneau et al., 2013). The poleward flow occupied the whole water column above 1000 m depth and extended to more than 80 km offshore. ~~In contrary, climatological poleward velocities associated with the PCUC at 12 °S are about 0.1 ms⁻¹ (Chaigneau et al., 2013). Similar values of average poleward flow have been reported from regional ocean models (e.g. Montes et al., 2010; Echevin et al., 2014) and from earlier observational data (e.g. Huyer et al., 1991; Czeschel et al., 2011).~~

The elevated poleward velocities at the eastern boundary were likely associated with a passing downwelling CTW. Satellite SLA data indicated a poleward propagation of a positive SLA signal from the equator to beyond 14 °° S that occurred simultaneously to the ~~intensified~~increase of poleward flow at 12 °° S. The SLA signal propagated at a speed consistent with the phase speed of the first vertical mode CTW. Similarly, the vertical distribution of the poleward velocity anomaly at the boundary was consistent with the cross-shore-depth velocity structure of a first vertical mode CTW.

Previous studies have identified the first vertical mode CTWs to dominate intraseasonal variability in the eastern South Pacific based on observations (Brink, 1982; Shaffer et al., 1997) and model results (Illig et al., 2018b). However, observed intraseasonal intensification of poleward flow within the depth range of the PCUC in a previous study by Pietri et al. (2014) was attributed to ~~a~~the second and third ~~vertical~~ mode CTW~~ modes~~. They found poleward velocities ~~long~~along the Peruvian continental slope increasing to ~~40 cm~~0.4 m s⁻¹.

Although the observed cross-shore-depth velocity structure of the CTW generally agrees with the first vertical mode solution of a linear wave model using local stratification and topography, there is disagreement in the details of the flow structure. ~~Certainly, as also~~It was noted ~~by Pietri et al. (2014), we are comparing~~previously that observed ~~velocities to~~velocity ~~anomalies caused by CTWs, thus~~structures agree poorly (Brink, 1982). Additionally, we compare only the theoretical modal structures with the difference between two velocity phases and the initial phase is no solid estimate of the mean alongshore circulation off Peru. Another possible explanation of the poor agreement between the first mode CTW and the observed ~~velocity~~ flow intensification is interaction of the CTW with local topography. North of our sampling site, the continental slope bends offshore at depths between 500 m to 1000 m (Fig. 1, insert) while the shelf narrows to the south. Changes in coastline, shelf width, and along-slope bathymetry lead to a transfer of CTW energy into higher modes (scattering) and upstream backscattering (Wang, 1980; Wilkin and Chapman, 1990; Kämpf (2018); Brunner et al., 2019). The influence of changes in shelf width on the upstream alongshore flow structure can ~~deviate from the wave solutions due to~~extend to 200 km upstream (Wilkin and Chapman, 1990) and is likely not relevant here. However, the bent of the continental slope north of out sampling site may stimulate energy transfer into high vertical mode CTWs. In turn, the superposition of ~~mean flow in the observations.~~several vertical modes could explain the observed elevated poleward flow between 50 m and 300 m depth. In fact, a recent model study suggests that differences between the theoretical CTW solutions and observations are predominately due to wave scattering (Brunner et al., 2019).

Furthermore, a recent study ~~shows~~suggests that differences between the theoretical CTW solutions and observations are due to wave scattering ~~not included in the wave~~into a greater proportion of higher-order modes or backscattering upstream (Brunner et al., 2019). Scattering occurs when a propagating CTW encounters changes in coastline, shelf width, and bathymetry. These changes were neglected when deriving the CTW mode solutions ~~presented here (Brunner et al., 2019, in press).~~used here.

The SLA data indicate that the first vertical CTW mode ~~CTW~~ along the eastern boundary that arrived at our sampling site in mid-May originated in the eastern equatorial Pacific at around 95° W. (Fig. 6). A coherent signal from this region propagated eastwards along the equator and arrived at about the same time when the equatorial SLA maximum at the coast was developing. The wind data shows a possible forcing of this wave around 160° W in early April by a weakening of zonal wind (Fig. 7a). This ~~suggested generation site~~ is ~~further to the east than that of most previously reported intraseasonal waves. In~~consistent with a recent comprehensive study ~~by~~ (Rydbeck et al. ~~(.,~~ 2019) identifying wind forcing variability west of 150° W ~~was found to be~~as the main generation mechanism of intraseasonal equatorial Kelvin waves. ~~ASCAT (Bentamy and Fillon, 2012) wind stress data shows a reduction of easterly winds at the equator in the region around 95 °W by about 2 m s⁻¹ while~~

570 However, in the SLA ~~anomaly is developing there. Furthermore, along shore winds speed at 12 °S off Peru reduce by 4 - 5 m s⁻¹ about a week prior to the arrival~~ the wave has an expression on east of 95° W compared to 150° W where Rydbeck et al. (2019) have located the maximum ~~SLA (not shown). This suggests that~~ of SLA signal. The location of the SLA signal to the eastern equatorial Pacific may have been caused by the negative SLA further in the ~~remotely forced downwelling CTW was reinforced by a local reduction of upwelling favourable winds~~west which reduces the positive SLA to an extent where it is no longer identifiable.

575 The temperature and salinity conditions on the shelf remain almost unchanged despite the strongly intensified poleward flow and are only displaced downwards, suggesting that the same water mass was advected within the boundary current regime during both observational periods. The weak warming and increase in salinity ~~are in agreement~~agree with ~~an~~the advection of the slightly warmer and saltier water along the PCUC path north of 12 ~~°~~° S (Grados et al., 2018). However, the signals are rather weak therefore we cannot relate them clearly to the circulation change. The SST declines despite the downwelling wave

580 which would be expected to cause warming. A downwelling CTW in March 2017 indeed has contributed to the warm SST anomalies (Echevin et al., 2018). However, the impact of CTWs on intraseasonal SST variability off Peru is limited in general (Dewitte et al., 2011; Illig et al., 2014). Specifically, in May 2017 SST reduction ~~is in agreement~~agrees with both the seasonal cycle (Graco et al., 2017) and the decline of the warm Coastal El Niño with peak SST in March (e.g. Garreaud, 2018).

Despite being non-conservative, the changes in oxygen concentrations are small as well. Only in the bottom water on the upper

585 continental slope, higher oxygen concentrations are displaced downwards. Faster advection should cause higher oxygen concentrations, because the time is shorter, in which oxygen is consumed by respiration along the PCUC path. Espinoza-Morriberón et al. (2019) attribute some of the oxygen variability associated with El Niño-Southern Oscillation to the changes in microbial respiration because advection speed and pathways change under El Niño conditions (e.g. Montes et al., 2011; Espinoza-Morriberón et al., 2017). However, Zamora et al. (2012) reported uniform oxygen concentrations for waters in the

590 PCUC; therefore, there is no oxygen change due to changes in alongshore advection, explaining the weak oxygen change in our study.

The limited impact of the CTW on oxygen may be related to high oxygen concentrations present at the study site before the wave passage. Compared to time series data of Callao (Graco et al., 2017) the concentrations were in the upper range of variability observed after the 1997-98 El Niño event. The 22 µmol kg⁻¹ surface was located at 50 m instead of 30 m reported

595 for the climatological state by Espinoza-Morriberón et al. (2019). Whether the higher oxygen concentrations are caused by the coastal El Niño event, in the same way that canonical El Niños are related to enhanced oxygenation (e.g. Helly and Levin, 2004; Stramma et al., 2016; Espinoza-Morriberón et al., 2019), cannot be answered with our available observational data. Coastal time series off northern Peru show an oxygenation starting in February 2017 but only a weaker signal at 12 ~~°~~° S (ENFEN, 2017) while hydrographic profiles collected in early to mid-April at 11 and 14 ~~°~~° S feature a very shallow oxycline

600 (not shown). Therefore, it remains unclear whether the higher oxygen concentrations in late-April and May at 12 ~~°~~° S are a local or short-term phenomenon or indeed related to the coastal El Niño event.

The increase in nitrate concentrations and the reduced nitrogen deficit are likely caused by the shorter advection timescales in the intensified flow. The nitrate increase occurs within the ESSW range and waters with the same T-S properties are richer in nitrate after the PCUC increase (Fig. ~~7~~9), excluding changed advection pathways as a likely cause of the increased nitrate load.

605 ~~As~~Along the ESSW ~~is moving southward in~~ pathway within the PCUC~~, the N loss leads to an increasing deficit of nitrogen between~~ from the equator ~~and~~to 12° S, the ~~analysed section~~nitrogen deficit increases while nitrate concentrations decrease (Silva et al., 2009; Zamora et al., 2012~~).~~; Kalvelage et al., 2013).. The increasing nitrogen deficit is caused by the microbially facilitated reduction of nitrate, nitrite and ammonium to N₂ gas which occurs in anoxic waters during the consumption of organic matter (e.g. Kalvelage et al., 2013). The resulting nitrogen deficit accumulates with time during the poleward

610 advection. Thus, the intensified PCUC ~~transports waters~~increases the poleward advection of water with a lower nitrogen deficit ~~polewards~~. The possibility of this mechanism is tested by calculating the advection timescales from the equatorial

15

regime: the 12 °S section is about 1800 km alongshore distance away from the equator, the advection timescale for a velocity of ~~40 cm~~ 0.4 m s^{-1} is 52 days, compared to 160 days for a velocity of 0.13 ~~cm~~ m s^{-1}, approximately the climatological PCUC velocity (Chaigneau et al., 2013). Using an N-loss of 48 nmol N l^{-1}d^{-1} (combined anammox and denitrification rates in the coastal OMZ from Kalvelage et al. (2013)), 5.2 µmol N l^{-1} can be transformed during the longer advection timescale. This may explain the reduction of the nitrogen deficit by about 5 µmol N kg^{-1}, as observed throughout much of the PCUC core.

The sediments off Peru below the OMZ release phosphate into the water column (Noffke et al., 2012; Lomnitz et al., 2016) that also contributes to the nitrogen deficit. Shorter advection timescales lead to a reduced accumulation of benthic phosphate release and in fact phosphate concentrations decrease during the strong PCUC flow. However, the ~~parallel determination~~increase of nitrate (and the sum of inorganic nitrogen species ~~and~~) exceeds the phosphate ~~shows that~~decrease by a ratio higher than the nitrogen to phosphorus relation implied in equation 1. Therefore, changes ~~in~~of nitrate concentration dominate the reduction of the nitrogen deficit.

The increase of nitrate by the downwelling CTW implies that the change of alongshore advection with the increased flow is more important for the nitrate balance than ~~the~~ downwelling ~~itself~~. The downwelling would displace the nutricline and thus low nutrient surface water downwards, lowering nutrient concentrations, which is not observed. The decline of nitrate concentrations during El Niño events has been associated with the nutricline displacement due to downwelling CTWs on interannual timescales (Graco et al., 2017; Espinoza-Morriberón et al., 2017). However, focusing on intraseasonal timescales, Echevin et al. (2014) modelled an almost cancelling of horizontal and vertical (i.e. nutricline movement) advection and a fast mode CTW not impacting nutricline depth. In a model study in the Atlantic Ocean, where nitrate decreases poleward as well, it was shown that the total effect of CTWs on nitrate concentrations varies regionally due to a different balance of horizontal and vertical advection (Bachèlery et al., 2016), but the horizontal advection always led to an increase in nitrate.

The changes in redox state in the water column and especially the bottom water affect the biogeochemical cycling in the sediment as well. Because microbial storage of nitrate and nitrite by microorganisms in the sediment can sustain vigorous N turnover even in the absence of bottom water nitrate and nitrite (Dale et al., 2016; Sommer et al., 2016), episodic events of nitrogen supply can be associated with continuous benthic nitrogen cycling. The absence of nitrate supply due to the absence of CTWs over longer time periods favours the depletion of nitrate in the water column as observed by Sommer et al. (2016) and may lead ultimately to the development of sulfidic events (Schunck et al., 2013; Dale et al., 2017; Callbeck et al., 2018).

6 Conclusion

Based on ~~intensive~~extensive physical and biogeochemical sampling, we describe and analyse the evolution of circulation, hydrography and biogeochemistry off Peru in early 2017. Poleward velocities within the PCUC intensified far beyond the reported climatological mean in May. This increased flow occurs during a limited time period in May in between weaker poleward transport in April and late June. The propagation velocity of positive SLA along the equator and coastline ~~suggest~~suggests that the intensified current is caused by a poleward propagating downwelling CTW of the first baroclinic mode ~~excited~~forced around 160° W at ~~about 95 °W on~~ the equator that causes a positive SLA signal east of 95° W. The transition of the circulation from a weak poleward flow to strong poleward flow decreased the timescale of alongshore advection ~~of water~~ from the equatorial current regime to the study site at 12° S.

The downwelling CTW is not associated with strong vertical displacements of waters; instead the advection caused by the intensified PCUC is more important. ~~The reduction of~~For parameters without strong horizontal gradients, an increase in PCUC flow does not cause pronounced changes in the advection ~~timescale does not affect~~. In this study this applies to the conservative properties~~; therefore~~ temperature and salinity ~~changes~~ as well as for oxygen where alongshore gradients are ~~small. But~~weak (Zamora et al., 2012). For these parameters there are no large differences between both circulation phases that can be attributed clearly to the altered circulation. Yet concentrations of nutrients are ~~affected~~influenced by ~~the reduction of time available for~~

16

reduction or accumulation. This causesshorter transit times, being less altered by biogeochemical cycling. Thisleads to an increase of bioavailable nitrogen as less is lost in the OMZ by N loss processes. The nitrogen. and its biogeochemistry is strongly changed by the alteredincreased ratio of nitrogen to phosphorus caused byrelated to the increased advection due to the CTW...

On intraseasonal timescalesFor the period from April to May 2017, our study suggests an increase in nitrate levels due to the passage of an intraseasonal downwelling CTW which is opposite to. This contrasts with the decrease observed previously on interannual timescales bycaused by downwelling CTWs (Graco et al., 2017). This shows that the impact of CTWs on nutrient biogeochemistry is a complex balance between different factors, with potentially different outcome on different timescales. Analysing the processes associated with individual intraseasonal waves is also necessary to understand the interannual effect of CTWs, which is based on varying occurrence of such waves in different years.

The high variability of circulation, nutrients and the nitrogen deficit during our observations showsdemonstrates the need for temporally resolved sampling as an individual section recorded may be very different tofrom the situation onlya few weeks later. StudyingQuantification of intraseasonal variability likein CTWs and their impact is – other than in modelling studies (e.g. Echevin et al., 2014) – only possible by high temporally resolved sampling as done in our study or in the study by Pietri et al. (2014), which is limited to the circulation only, to be able to track the changes occurring within a few daysat high temporal resolution.

Data availability

Author contributions

Competing Interests

Acknowledgements

Many figures in this study use colour maps from the cmocean package (Thyng et al., 2016). Global Ocean Gridded L4 sea
690 surface heights were made available by E.U. Copernicus Marine Service (CMEMS).

References

Albert, A., Echevin, V., Lévy, M., and Aumont, O.: Impact of nearshore wind stress curl on coastal circulation and primary productivity in the Peru upwelling system, J. Geophys. Res. Oceans, 115. doi:10.1029/2010JC006569, 2010.

Bachèlery, M.-L., Illig, S., and Dadou, I.: Forcings of nutrient, oxygen, and primary production interannual variability in the
695 southeast Atlantic Ocean, Geophys. Res. Lett., 43, 8617-8625. doi:10.1002/2016gl070288, 2016.

Bakun, A. and Nelson, C. S.: The Seasonal Cycle of Wind-Stress Curl in Subtropical Eastern Boundary Current Regions, J. Phys. Oceanogr., 21, 1815-1834. doi:10.1175/1520-0485(1991)021<1815:TSCOWS>2.0.CO;2, 1991.

Belmadani, A., Echevin, V., Dewitte, B., and Colas, F.: Equatorially forced intraseasonal propagations along the Peru-Chile coast and their relation with the nearshore eddy activity in 1992–2000: A modeling study, J. Geophys. Res. Oceans, 117.
700 doi:10.1029/2011JC007848, 2012.

Bentamy, A. and Fillon, D. C.: Gridded surface wind fields from Metop/ASCAT measurements, Int. J. Remote Sens., 33, 1729-1754. doi:10.1080/01431161.2011.600348, 2012.

Brandt, P., Bange, H. W., Banyte, D., Dengler, M., Didwischus, S.-H., Fischer, T., Greatbatch, R. J., Hahn, J., Kanzow, T., Karstensen, J., Körtzinger, A., Krahmann, G., Schmidtko, S., Stramma, L., Tanhua, T., and Visbeck, M.: On the role of
705 circulation and mixing in the ventilation of oxygen minimum zones with a focus on the eastern tropical North Atlantic, Biogeosciences, 12, 489-512. doi:10.5194/bg-12-489-2015, 2015.

Brink, K. H.: A Comparison of Long Coastal Trapped Wave Theory with Observations off Peru, J. Phys. Oceanogr., 12, 897-913. doi:10.1175/1520-0485(1982)012<0897:ACOLCT>2.0.CO;2, 1982.

Brink, K. H.: Energy Conservation in Coastal-Trapped Wave Calculations, J. Phys. Oceanogr., 19, 1011-1016.
710 doi:10.1175/1520-0485(1989)019<1011:ECICTW>2.0.CO;2, 1989.

Brink, K. H.: Stable coastal-trapped waves with stratification, topography and mean flow, MBLWHOI Library. doi:10.1575/1912/10527, 2018.

Brink, K. H. and Chapman, D. C.: Programs for computing properties of coastal-trapped waves and wind-driven motions over the continental shelf and slope, WHOI Technical Reports, Woods Hole Oceanographic Institution. doi:10.1575/1912/5368,
715 1987.

Brink, K. H., Halpern, D., Huyer, A., and Smith, R. L.: The physical environment of the Peruvian upwelling system, Prog. Oceanogr., 12, 285-305. doi:10.1016/0079-6611(83)90011-3, 1983.

Brunner, K., Rivas, D. and Lwiza, K. M. M.: Application of ~~classical coastal trapped wave theory~~Classical Coastal Trapped Wave Theory to ~~high scattering regions~~High-Scattering Regions, J. Phys. Oceanogr., 49(9), 2201–2216, doi:10.1175/JPO-D-
720 18-0112.1, 2019~~, in press~~.

Callbeck, C. M., Lavik, G., Ferdelman, T. G., Fuchs, B., Gruber-Vodicka, H. R., Hach, P. F., Littmann, S., Schoffelen, N. J., Kalvelage, T., Thomsen, S., Schunck, H., Löscher, C. R., Schmitz, R. A., and Kuypers, M. M. M.: Oxygen minimum zone cryptic sulfur cycling sustained by offshore transport of key sulfur oxidizing bacteria, Nat. Commun., 9. doi:10.1038/s41467-018-04041-x, 2018.

725 Carr, M.-E.: Estimation of potential productivity in Eastern Boundary Currents using remote sensing, Deep Sea Res. Part II, 49, 59-80. doi:10.1016/S0967-0645(01)00094-7, 2002.

Chaigneau, A., Dominguez, N., Eldin, G., Vasquez, L., Flores, R., Grados, C., and Echevin, V.: Near-coastal circulation in the Northern Humboldt Current System from shipboard ADCP data, J. Geophys. Res. Oceans, 118, 5251-5266. doi:10.1002/jgrc.20328, 2013.

730 Chang, B. X., Devol, A. H., and Emerson, S. R.: Denitrification and the nitrogen gas excess in the eastern tropical South Pacific oxygen deficient zone, Deep Sea Res. Part I, 57, 1092-1101. doi:10.1016/j.dsr.2010.05.009, 2010.

Chavez, F. P., Bertrand, A., Guevara-Carrasco, R., Soler, P., and Csirke, J.: The northern Humboldt Current System: Brief history, present status and a view towards the future, Prog. Oceanogr., 79, 95-105. doi:10.1016/j.pocean.2008.10.012, 2008.

Codispoti, L. A.: An oceanic fixed nitrogen sink exceeding 400 Tg N a^{-1} vs the concept of homeostasis in the fixed-nitrogen

735 inventory, Biogeosciences, 4, 233-253. doi:10.5194/bg-4-233-2007, 2007.

~~Czeschel, R.,~~Colas, F., Capet, X., McWilliams, J. C. and Shchepetkin, A.: 1997–1998 El Niño off Peru: A numerical study, Prog. Oceanogr., 79(2–4), 138–155, doi:10.1016/j.pocean.2008.10.015, 2008.

Cornejo-Rodriguez, M. D. P. and Enfield, D. B.: Propagation and forcing of high-frequency sea level variability along the west coast of South America, J. Geophys. Res. Oceans, 92(C13), 14323–14334, doi:10.1029/JC092iC13p14323,

740 1987.Czeschel, R., Stramma, L., Schwarzkopf, F. U., Giese, B. S., Funk, A., and Karstensen, J.: Middepth circulation of the eastern tropical South Pacific and its link to the oxygen minimum zone, J. Geophys. Res. Oceans, 116. doi:10.1029/2010JC006565, 2011.

Dale, A. W., Graco, M., and Wallmann, K.: Strong and Dynamic Benthic-Pelagic Coupling and Feedbacks in a Coastal Upwelling System (Peruvian Shelf), Front. Mar. Sci. 4:29, doi.org/10.3389/fmars.2017.00029, 2017.

745 Dale, A. W., Sommer, S., Lomnitz, U., Bourbonnais, A., and Wallmann, K.: Biological nitrate transport in sediments on the Peruvian margin mitigates benthic sulfide emissions and drives pelagic N loss during stagnation events, Deep Sea Res. Part I, 112, 123-136. doi:10.1016/j.dsr.2016.02.013, 2016.

Dengler, M. and Sommer, S.: Coupled benthic and pelagic oxygen, nutrient and trace metal cycling, ventilation and carbon degradation in the oxygen minimum zone of the Peruvian continental margin (SFB 754): Cruise No. M 136 11.04. - 03.05.2017

750 Callao (Peru) - Callao Solute-Flux Peru I, METEOR-Berichte, doi:10.3289/CR_M136, 2017.

DeVries, T., Deutsch, C., Rafter, P. A., and Primeau, F.: Marine denitrification rates determined from a global 3-D inverse model, Biogeosciences, 10, 2481-2496. doi:10.5194/bg-10-2481-2013, 2013.

Dewitte, B., Illig, S., Renault, L., Goubanova, K., Takahashi, K., Gushchina, D., Mosquera, K. and Purca, S.: Modes of covariability between sea surface temperature and wind stress intraseasonal anomalies along the coast of Peru from satellite

755 observations (2000–2008), J. Geophys. Res. Oceans, 116(C4), doi:10.1029/2010JC006495, 2011.

Echevin, V., Albert, A., Lévy, M., Graco, M., Aumont, O., Piétri, A., and Garric, G.: Intraseasonal variability of nearshore productivity in the Northern Humboldt Current System: The role of coastal trapped waves, Cont. Shelf Res., 73, 14-30. doi:10.1016/j.csr.2013.11.015, 2014.

Echevin, V., Colas, F., Espinoza-Morriberon, D., Vasquez, L., Anculle, T., and Gutierrez, D.: Forcings and Evolution of the

760 2017 Coastal El Niño Off Northern Peru and Ecuador, Front. Mar. Sci., 5, 367. doi:10.3389/fmars.2018.00367, 2018.

ENFEN: Technical Report ENFEN no 3 2017, Comité Multisectorial encargado del Estudio Nacional del Fenómeno El Niño (Enfen). [online] Available from: https://www.dhn.mil.pe/Archivos/oceanografia/enfen/informe-tecnico/03-2017.pdf, 2017.

Enfield, D. B., Cornejo-Rodriguez, M. D., Smith, R. L., and Newberger, P. A.: The equatorial source of propagating variability along the Peru coast during the 1982–1983 El Niño, J. Geophys. Res. Oceans, 92, 14335-14346.

765 doi:10.1029/JC092iC13p14335, 1987.

Espinoza-Morriberón, D., Echevin, V., Colas, F., Tam, J., Gutierrez, D., Graco, M., Ledesma, J. and Quispe-Ccalluari, C.: Oxygen Variability During ENSO in the Tropical South Eastern Pacific, Front. Mar. Sci., 5, 526, doi:10.3389/fmars.2018.00526, 2019.

Espinoza-Morriberón, D., Echevin, V., Colas, F., Tam, J., Ledesma, J., Vásquez, L., and Graco, M.: Impacts of El Niño events

770 on the Peruvian upwelling system productivity, J. Geophys. Res. Oceans. doi:10.1002/2016JC012439, 2017.

Fennel, W., Junker, T., Schmidt, M. and Mohrholz, V.: Response of the Benguela upwelling systems to spatial variations in the wind stress, Cont. Shelf Res., 45, 65–77, doi:10.1016/j.csr.2012.06.004, 2012.Fischer, J., Brandt, P., Dengler, M., Müller,

M., and Symonds, D.: Surveying the Upper Ocean with the Ocean Surveyor: A New Phased Array Doppler Current Profiler, J. Atmos. Oceanic Technol., 20, 742-751. doi:10.1175/1520-0426(2003)20<742:STUOWT>2.0.CO;2, 2003.

775 Garreaud, R. D.: A plausible atmospheric trigger for the 2017 coastal El Niño, Int. J. Climatol., 38, e1296-e1302. doi:10.1002/joc.5426, 2018.

Graco, M. I., Purca, S., Dewitte, B., Castro, C. G., Morón, O., Ledesma, J., Flores, G. and Gutiérrez, D.: The OMZ and nutrient features as a signature of interannual and low-frequency variability in the Peruvian upwelling system, Biogeosciences, 14(20), 4601–4617, doi:10.5194/bg-14-4601-2017, 2017.

780 Grados, C., Chaigneau, A., Echevin, V., and Dominguez, N.: Upper ocean hydrology of the Northern Humboldt Current System at seasonal, interannual and interdecadal scales, Prog. Oceanogr., 165, 123-144. doi:10.1016/j.pocean.2018.05.005, 2018.

Grasshoff, K., Kremling, K. and Ehrhardt, M.: Methods of seawater analysis, John Wiley & Sons., 1983.

Gruber, N.: The Dynamics of the Marine Nitrogen Cycle and its Influence on Atmospheric CO2 Variations, in The Ocean
785 Carbon Cycle and Climate, edited by M. Follows and T. Oguz, pp. 97–148, Springer Netherlands, Dordrecht., 2004.

Gruber, N. and Sarmiento, J. L.: Global patterns of marine nitrogen fixation and denitrification, Global Biogeochem. Cycles, 11, 235-266. doi:10.1029/97GB00077, 1997

Gunther, E. R.: A report on oceanographical investigations in the Peru Coastal Current, Discovery Rep., 13, 107–276, 1936.

Gutiérrez, D., Enríquez, E., Purca, S., Quipúzcoa, L., Marquina, R., Flores, G. and Graco, M.: Oxygenation episodes on the
790 continental shelf of central Peru: Remote forcing and benthic ecosystem response, Prog. Oceanogr., 79(2–4), 177–189, doi:10.1016/j.pocean.2008.10.025, 2008.

Helly, J. J. and Levin, L. A.: Global distribution of naturally occurring marine hypoxia on continental margins, Deep Sea Res. Part I, 51, 1159-1168. doi:10.1016/j.dsr.2004.03.009, 2004.

Hill, A. E., Hickey, B. M., Shillington, F. A., Strub, P. T., Brink, K. H., Barton, E. D. and Thomas, A. C.: Eastern Ocean
795 Boundaries, in The Seas: The Global Coastal Ocean, vol. 11, edited by A. R. Robinson and K. H. Brink, pp. 29–68, John Wiley, New York., 1998.

Holmes, R. M., Aminot, A., Kérouel, R., Hooker, B. A., and Peterson, B. J.: A simple and precise method for measuring ammonium in marine and freshwater ecosystems, Can. J. Fish. Aquat.Sci., 56, 1801-1808. doi:10.1139/f99-128, 1999.

Hormazabal, S., Shaffer, G., and Pizarro, O.: Tropical Pacific control of intraseasonal oscillations off Chile by way of oceanic
800 and atmospheric pathways, Geophys. Res. Lett., 29. doi:10.1029/2001GL013481, 2002.

~~Huyer, A., Knoll, M.,~~Huang, B., Thorne, P. W., Banzon, V. F., Boyer, T., Chepurin, G., Lawrimore, J. H., Menne, M. J., Smith, T. M., Vose, R. S. and Zhang, H.-M.: NOAA Extended Reconstructed Sea Surface Temperature (ERSST), Version 5, doi:10.7289/V5T72FNM, 2017a.

Huang, B., Thorne, P. W., Banzon, V. F., Boyer, T., Chepurin, G., Lawrimore, J. H., Menne, M. J., Smith, T. M., Vose, R. S.
805 and Zhang, H.-M.: Extended Reconstructed Sea Surface Temperature, Version 5 (ERSSTv5): Upgrades, Validations, and Intercomparisons, J. Climate, 30(20), 8179–8205, doi:10.1175/JCLI-D-16-0836.1, 2017b.Huyer, A., Knoll, M., Paluszkiewicz, T., and Smith, R. L.: The Peru Undercurrent: a study in variability, Deep-Sea Res., 38, Supplement 1, S247 - S271. doi:10.1016/S0198-0149(12)80012-4, 1991.

Illig, S., Bachèlery, M.-L., and Cadier, E.: Subseasonal Coastal-Trapped Wave Propagations in the Southeastern Pacific and
810 Atlantic Oceans: 2. Wave Characteristics and Connection With the Equatorial Variability, J. Geophys. Res. Oceans, 123, 3942-3961. doi:10.1029/2017JC013540, 2018b.

Illig, S., Cadier, E., Bachèlery, M.-L., and Kersalé, M.: Subseasonal Coastal-Trapped Wave Propagations in the Southeastern Pacific and Atlantic Oceans: 1. A New Approach to Estimate Wave Amplitude, J. Geophys. Res. Oceans, 123, 3915-3941. doi:10.1029/2017JC013539, 2018a

815 Illig, S., Dewitte, B., Goubanova, K., Cambon, G., Boucharel, J., Monetti, F., Romero, C., Purca, S. and Flores, R.: Forcing mechanisms of intraseasonal SST variability off central Peru in 2000–2008, J. Geophys. Res. Oceans, 119(6), 3548–3573, doi:10.1002/2013JC009779, 2014.

IOC, SCOR and IAPSO: The international thermodynamic equation of seawater – 2010: Calculation and use of thermodynamic properties, edited by U. (english), Intergovernmental Oceanographic Commission., 2010.

820 ~~Kalvelage, T., Lavik, G.,~~Junker, T., Schmidt, M. and Mohrholz, V.: The relation of wind stress curl and meridional transport in the Benguela upwelling system, J. Mar. Syst., 143, 1–6, doi:10.1016/j.jmarsys.2014.10.006, 2015.Kalvelage, T., Lavik, G., Lam, P., Contreras, S., Arteaga, L. and L&ouml: Nitrogen cycling driven by organic matter export in the South Pacific oxygen minimum zone, Nat. Geosci., 6(3), 228–234, doi:10.1038/ngeo1739, 2013.

Kämpf, J. and Chapman, P.: Upwelling Systems of the World: A Scientific Journey to the Most Productive Marine Ecosystems,
825 Springer, 2016.

Karstensen, J., Schütte, F., Pietri, A., Krahmann, G., Fiedler, B., Grundle, D., Hauss, H., Körtzinger, A., Löscher, C. R., Testor, P., Vieira, N. and Visbeck, M.: Upwelling and isolation in oxygen-depleted anticyclonic modewater eddies and implications for nitrate cycling, Biogeosciences, 14(8), 2167–2181, doi:10.5194/bg-14-2167-2017, 2017.

Karstensen, J., Stramma, L., and Visbeck, M.: Oxygen minimum zones in the eastern tropical Atlantic and Pacific oceans,
830 Prog. Oceanogr., 77, 331-350. doi:10.1016/j.pocean.2007.05.009, 2008.

Klenz, T., Dengler, M., and Brandt, P.: Seasonal Variability of the Mauritania Current and Hydrography at 18°_N, J. Geophys. Res. Oceans, 123, 8122-8137. doi:10.1029/2018jc014264, 2018.

~~Lomnitz, U.,~~Leth, O. and Middleton, J. F.: A numerical study of the upwelling circulation off central Chile: Effects of remote oceanic forcing, J. Geophys. Res. Oceans, 111(C12), doi:10.1029/2005JC003070, 2006.Lomnitz, U., Sommer, S., Dale, A.
835 W., Löscher, C. R., Noffke, A., Wallmann, K., and Hensen, C.: Benthic phosphorus cycling in the Peruvian oxygen minimum zone, Biogeosciences, 13, 1367-1386. doi:10.5194/bg-13-1367-2016, 2016.

~~McCreary, J.~~Marchesiello, P., McWilliams, J. C. and Shchepetkin, A.: Equilibrium Structure and Dynamics of the California Current System, J. Phys. Oceanogr., 33(4), 753–783, doi: 10.1175/1520-0485(2003)33<753:ESADOT>2.0.CO;2, 2003.McCreary, J. P. and Chao, S.-Y.: Three-dimensional shelf circulation along an eastern ocean boundary, J. Mar. Res., 43,
840 13-36. doi:10.1357/002224085788437316, 1985.

~~McDougall, T.~~McCreary, J. P., Kundu, P. K. and Chao, S.-Y.: On the dynamics of the California Current system, J. Mar. Res., 45(1), 1–32, doi:10.1357/002224087788400945, 1987.McDougall, T. J. and Barker, P. M.: Getting started with TEOS-10 and the Gibbs Seawater (GSW) oceanographic toolbox, SCOR/IAPSO WG 127, 2011.

Montes, I., Colas, F., Capet, X., and Schneider, W.: On the pathways of the equatorial subsurface currents in the eastern
845 equatorial Pacific and their contributions to the Peru-Chile Undercurrent, J. Geophys. Res. Oceans, 115. doi:10.1029/2009JC005710, 2010.

Montes, I., Schneider, W., Colas, F., Blanke, B., and Echevin, V.: Subsurface connections in the eastern tropical Pacific during La Niña 1999–2001 and El Niño 2002–2003, J. Geophys. Res. Oceans, 116. doi:10.1029/2011JC007624, 2011.

Moore, D. W. and Philander, S. G. H.: Modelling of the tropical ocean circulation, in The Sea, vol. 6, pp. 316–361, John
850 Wiley., 1977.

Noffke, A., Hensen, C., Sommer, S., Scholz, F., Bohlen, L., Mosch, T., Graco, M. and Wallmann, K.: Benthic iron and phosphorus fluxes across the Peruvian oxygen minimum zone, Limnol. Oceanogr., 57(3), 851–867, doi:10.4319/lo.2012.57.3.0851, 2012.

Paulmier, A. and Ruiz-Pino, D.: Oxygen minimum zones (OMZs) in the modern ocean, Prog. Oceanogr., 80, 113-128.
855 doi:10.1016/j.pocean.2008.08.001, 2009.

Pennington, J. T., Mahoney, K. L., Kuwahara, V. S., Kolber, D. D., Calienes, R., and Chavez, F. P.: Primary production in the eastern tropical Pacific: A review, Prog. Oceanogr., 69, 285-317. doi:10.1016/j.pocean.2006.03.012, 2006.

Penven, P., Echevin, V., Pasapera, J., Colas, F., and Tam, J.: Average circulation, seasonal cycle, and mesoscale dynamics of the Peru Current System: A modeling approach, J. Geophys. Res. Oceans, 110. doi:10.1029/2005JC002945, 2005.

860   Philander, S. G. H. and Yoon, J.-H.: Eastern Boundary Currents and Coastal Upwelling, J. Phys. Oceanogr., 12(8), 862–879, doi:10.1175/1520-0485(1982)012<0862:EBCACU>2.0.CO;2, 1982.

Pietri, A., Echevin, V., Testor, P., Chaigneau, A., Mortier, L., Grados, C., and Albert, A.: Impact of a coastal-trapped wave on the near-coastal circulation of the Peru upwelling system from glider data, J. Geophys. Res. Oceans, 119, 2109-2120. doi:10.1002/2013JC009270, 2014.

865   Pizarro, O., Shaffer, G., Dewitte, B., and Ramos, M.: Dynamics of seasonal and interannual variability of the Peru-Chile Undercurrent, Geophys. Res. Lett., 29, 22-1 - 22-4. doi:10.1029/2002GL014790, 2002.

Ramos, M., Dewitte, B., Pizarro, O., and Garric, G.: Vertical propagation of extratropical Rossby waves during the 1997-1998 El Niño off the west coast of South America in a medium-resolution OGCM simulation, J. Geophys. Res., 113. doi:10.1029/2007jc004681, 2008.

870   Revsbech, N. P., Larsen, L. H., Gundersen, J., Dalsgaard, T., Ulloa, O., and Thamdrup, B.: Determination of ultra-low oxygen concentrations in oxygen minimum zones by the STOX sensor, Limnol. Oceanogr. Methods, 7, 371-381. doi:10.4319/lom.2009.7.371, 2009.

Rydbeck, A. V., Jensen, T. G., and Flatau, M.: Characterization of Intraseasonal Kelvin Waves in the Equatorial Pacific Ocean, J. Geophys. Res. Oceans, 124, 2028-2053. doi:10.1029/2018jc014838, 2019.

875   Sakamoto, C. M., Johnson, K. S., and Coletti, L. J.: Improved algorithm for the computation of nitrate concentrations in seawater using an in situ ultraviolet spectrophotometer, Limnol. Oceanogr. Methods, 7, 132-143. doi:10.4319/lom.2009.7.132, 2009.

Schunck, H., Lavik, G., Desai, D. K., Großkopf, T., Kalvelage, T., Löscher, C. R., Paulmier, A., Contreras, S., Siegel, H., Holtappels, M., Rosenstiel, P., Schilhabel, M. B., Graco, M., Schmitz, R. A., Kuypers, M. M. M. and LaRoche, J.: Giant

880   Hydrogen Sulfide Plume in the Oxygen Minimum Zone off Peru Supports Chemolithoautotrophy, PLoS One, 8(8), 1–18, doi:10.1371/journal.pone.0068661, 2013.

Shaffer, G., Pizarro, O., Djurfeldt, L., Salinas, S., and Rutllant, J. (1997). Circulation and Low-Frequency Variability near the Chilean Coast: Remotely Forced Fluctuations during the 1991–92 El Niño, Journal of Physical Oceanography, 27, 217-235. doi:10.1175/1520-0485(1997)027<0217:CALFVN>2.0.CO;2, 1997.

885   Silva, N., Rojas, N., and Fedele, A.: Water masses in the Humboldt Current System: Properties, distribution, and the nitrate deficit as a chemical water mass tracer for Equatorial Subsurface Water off Chile, Deep Sea Res. Part II, 56, 1004-1020. doi:10.1016/j.dsr2.2008.12.013, 2009.

Sommer, S., Gier, J., Treude, T., Lomnitz, U., Dengler, M., Cardich, J., and Dale, A. W.: Depletion of oxygen, nitrate and nitrite in the Peruvian oxygen minimum zone cause an imbalance of benthic nitrogen fluxes, Deep Sea Res. Part I, 112, 113-

890   122. doi:10.1016/j.dsr.2016.03.001, 2016.

Sommer, S., Dengler, M. and Shipboard Scientific Party.: Benthic element cycling, fluxes and transport of nutrients and trace metals across the benthic boundary layer in the Peruvian oxygen minimum zone (SFB 754), Cruise No. 137, 06.05. - 29.05.2017, Callao (Peru) - Callao, METEOR-Berichte, doi:10.2312/cr_m137, 2019.

Stramma, L., Fischer, T., Grundle, D. S., Krahmann, G., Bange, H. W., and Marandino, C. A.: Observed El Niño conditions

895   in the eastern tropical Pacific in October 2015, Ocean Sci., 12, 861-873. doi:10.5194/os-12-861-2016, 2016.

Strub, P. T., Mesias, J. M., Montecino, V., Rutllant, J. and Salinas, S.: Coastal ocean circulation off western South America, in The Seas: The Global Coastal Ocean, vol. 11, edited by A. R. Robinson and K. H. Brink, pp. 273–313, John Wiley, New York., 1998.

Thomsen, S., Kanzow, T., Krahmann, G., Greatbatch, R. J., Dengler, M., and Lavik, G.: The formation of a subsurface anticyclonic eddy in the Peru-Chile Undercurrent and its impact on the near-coastal salinity, oxygen, and nutrient distributions, J. Geophys. Res. Oceans, 121, 476-501. doi:10.1002/2015JC010878, 2016.

Thomsen, S., Karstensen, J., Kiko, R., Krahmann, G., Dengler, M., and Engel, A.: Remote and local drivers of oxygen and nitrate variability in the shallow oxygen minimum zone off Mauritania in June 2014, Biogeosciences, 16, 979-998. doi:10.5194/bg-16-979-2019, 2019.

Thyng, K. M., Greene, C. A., Hetland, R. D., Zimmerle, H. M. and DiMarco, S. F.: True Colors of Oceanography: Guidelines for Effective and Accurate Colormap Selection, Oceanography, 29, doi:10.5670/oceanog.2016.66, 2016.

Ulloa, O., Canfield, D. E., DeLong, E. F., Letelier, R. M. and Stewart, F. J.: Microbial oceanography of anoxic oxygen minimum zones, Proceedings of the National Academy of Sciences, 109(40), 15996–16003, doi:10.1073/pnas.1205009109, 2012.

Wang, W.-L., Moore, J. K., Martiny, A. C. and Primeau, F. W.: Convergent estimates of marine nitrogen fixation, Nature, 566(7743), 205–211, doi:10.1038/s41586-019-0911-2, 2019.

Winkler, L. W.: Die Bestimmung des im Wasser gelösten Sauerstoffes, Ber. Dtsch. Chem. Ges., 21(2), 2843–2854, doi:10.1002/cber.188802102122, 1888.

-H. Yoon, J. and Philander, S. G. H.: The generation of coastal undercurrents, J. Oceanogr. Soc. Jpn., 38(4), 215–224, doi:10.1007/bf02111104, 1982.

Yu, X., and McPhaden, M. J.: Seasonal Variability in the Equatorial Pacific, J. Phys. Oceanogr., 29, 925-947. doi:10.1175/1520-0485(1999)029<0925:SVITEP>2.0.CO;2, 1999.

Zamora, L. M., Oschlies, A., Bange, H. W., Huebert, K. B., Craig, J. D., Kock, A., and Löscher, C. R.: Nitrous oxide dynamics in low oxygen regions of the Pacific: insights from the MEMENTO database, Biogeosciences, 9, 5007-5022. doi:10.5194/bg-9-5007-2012, 2012.

Zhang, W.and Lentz, S. J.: Wind-Driven Circulation in a Shelf Valley. Part I: Mechanism of the Asymmetrical Response to Along-Shelf Winds in Opposite Directions, J. Phys. Oceanogr., 47(12), 2927–2947, doi:10.1175/JPO-D-17-0083.1, 2017.
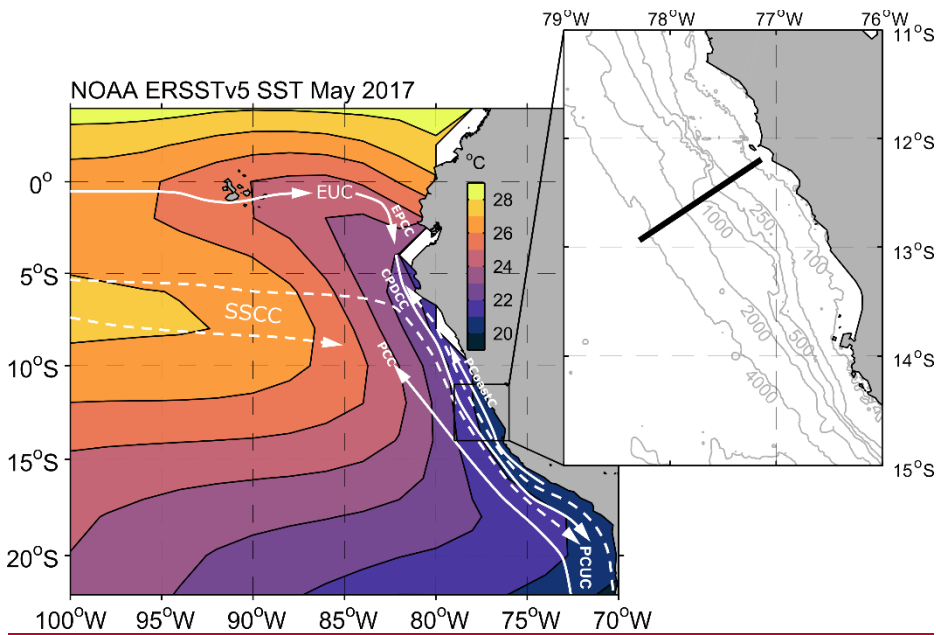
Table 1: Dates of R/V Meteor cruises conducted within the ETSP in 2017 including sampling time and number of CTD stations collected 12° S.

R/V Meteor cruise	Dates in 2017	Sampling duration along 12° S	CTD/nutrient stations at 12° S
M135	March 2 – April 8	2 days	
M136	April 18 – May 3	15 days	59 profiles
M137	May 6 – 29	23 days	92 profiles
M138	June 1 – July 5	1 day	
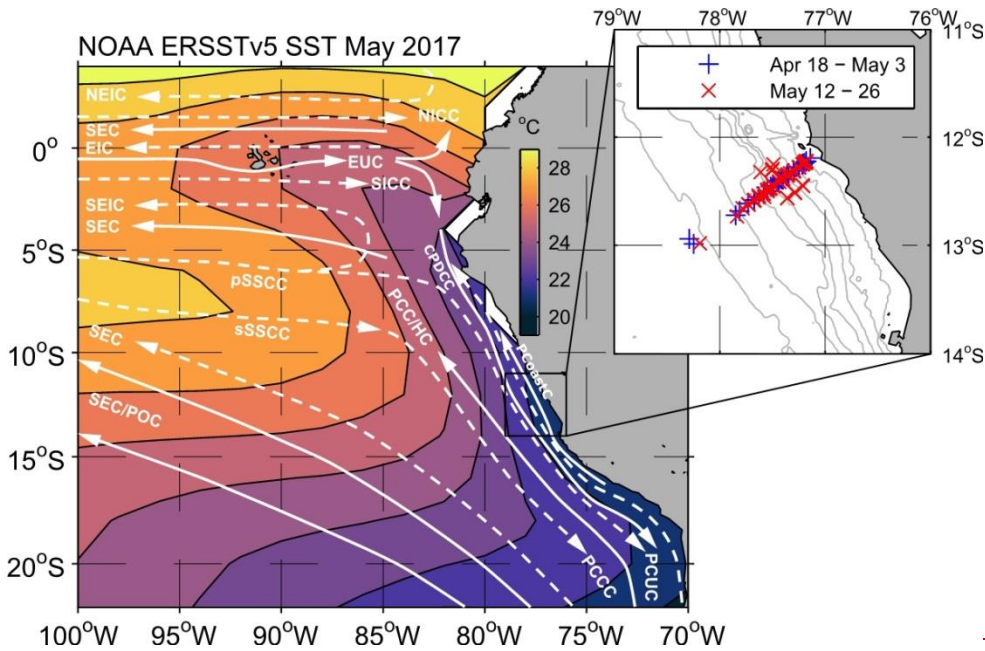
Figure 1: ~~Sea surface temperature (~~NOAA ERSSTv5 SST~~)~~ in ~~the eastern tropical Pacific during~~ May 2017~~, position of CTD profiles used along the 12°S Section in the insert. Current bands~~ and schematic of the circulation. White solid lines indicate surface layer currents while dashed lines indicate thermocline layer currents (after Brandt et al., 2015~~) overlaid).~~ Abbreviated currents are~~: for the surface layer (white solid arrows), the South Equatorial Current (SEC),~~ the Equatorial Undercurrent (EUC), the Ecuador-Peru Coastal Current (EPCC), the Peru Coastal Current (PCoastC), the Peru Chile ~~or Humboldt~~ Current (PCC~~/HC), the Peru Oceanic Current (POC), and for the thermocline layer (white dashed arrows), the North Equatorial Intermediate Current (NEIC), the North Intermediate Countercurrent (NICC), the Equatorial Intermediate Current (EIC), the South Intermediate Countercurrent (SICC), the primary and secondary~~), the Southern Subsurface Countercurrents (~~pSSCC, sSSCC~~SSCC, with two branches), the ~~deeper layer of the SEC, the~~ Chile–Peru Deep Coastal Current (CPDCC), and the Peru–Chile Undercurrent (PCUC~~) and the Peru–Chile Countercurrent (PCCC). Figure insert shows the position of the 12° S section and local bathymetry (SRTM30 plus topography, Becker et al., 2009).

26

950

27

955
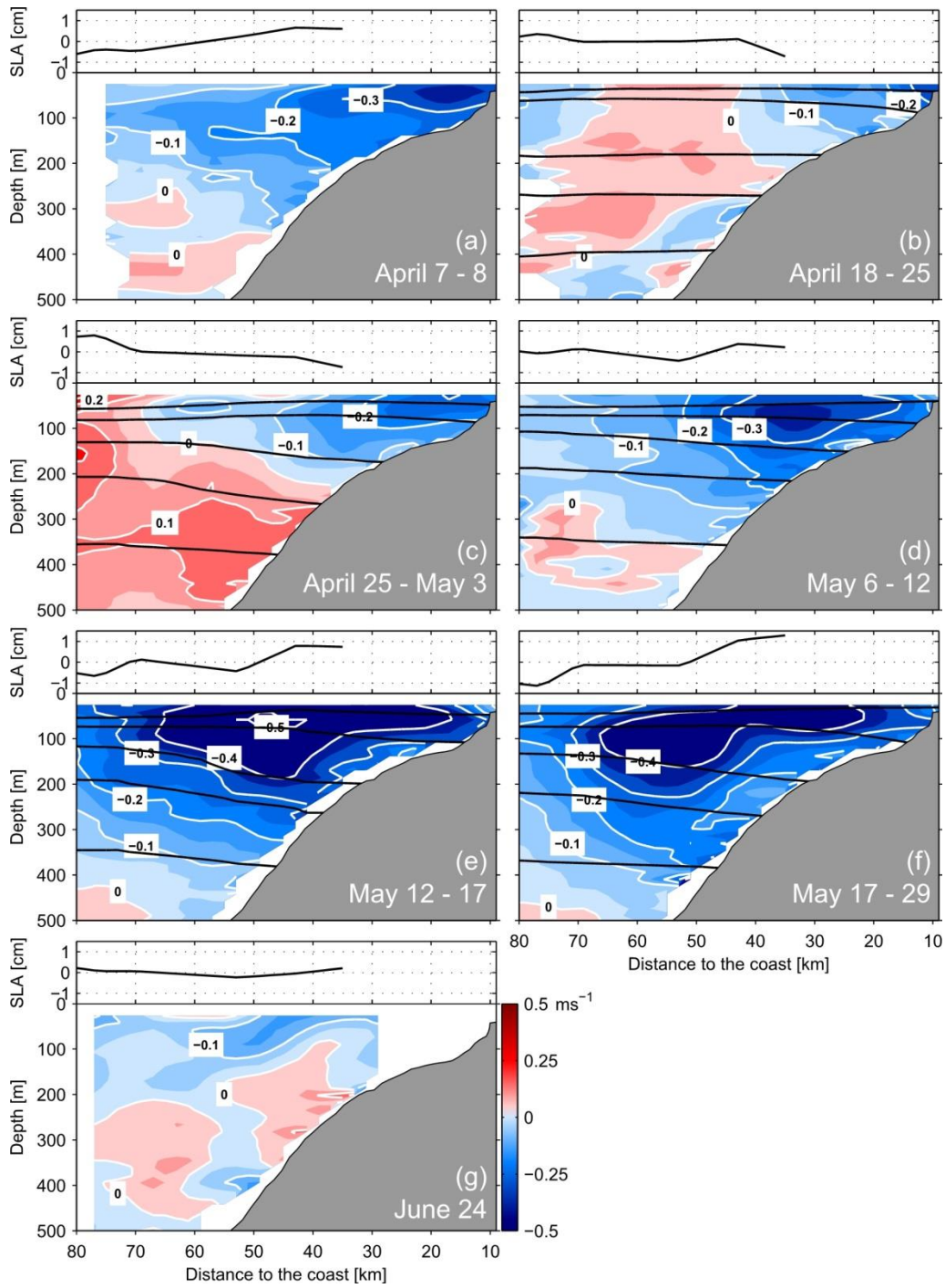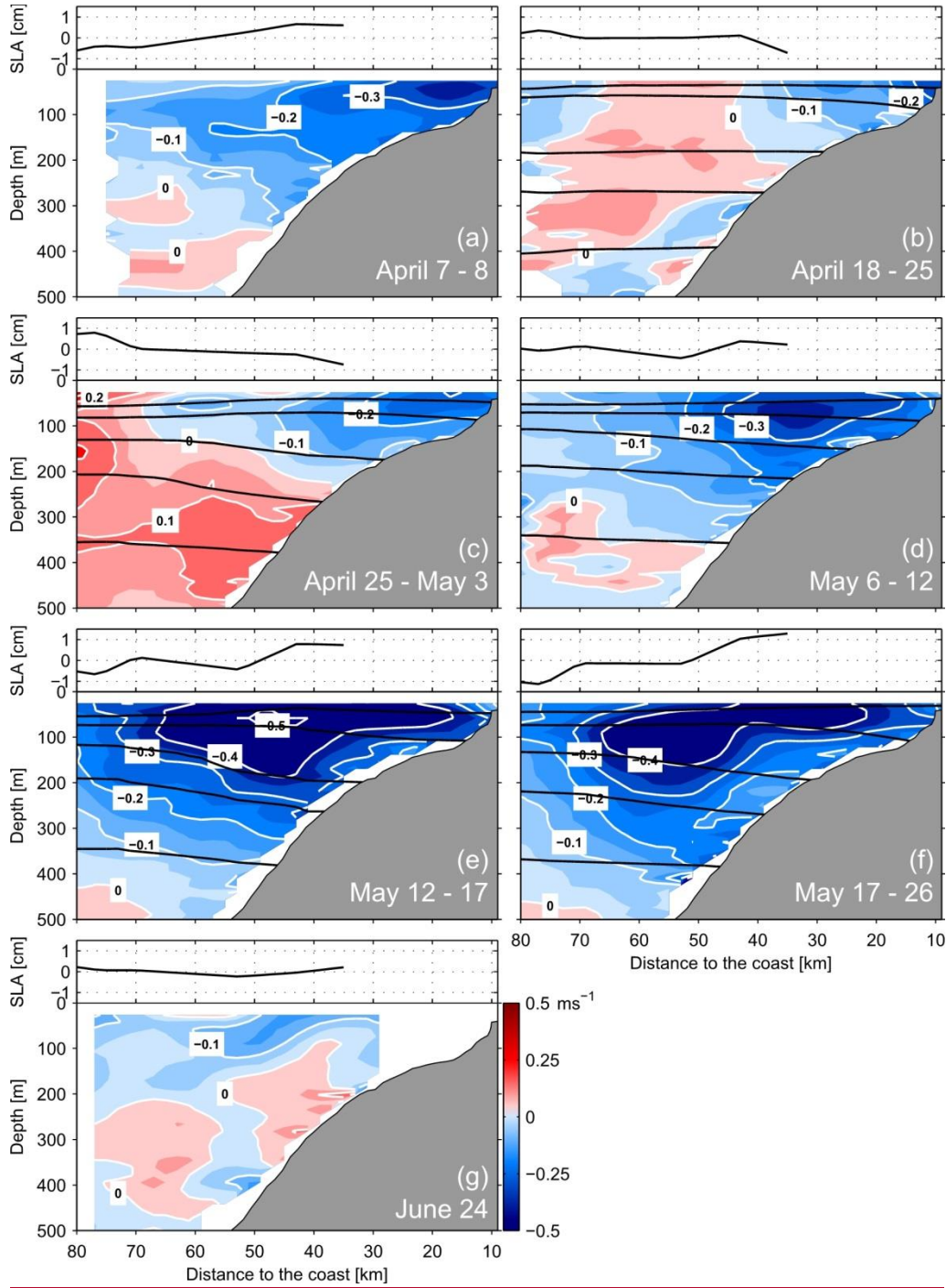
Figure 2: ~~Alongshore circulation at the 12 °S section off Peru from OS75 vmADCP shown in colour shading, the 25.6, 25.9, 26.2, 26.4,~~ Depth-distance distribution of alongshore velocity (in m s⁻¹, lower subpanels) ~~and 26.7 kg m⁻³ isopycnals in black, the SLA is shown in the~~ sea level anomaly (in cm, upper subpanels~~,~~) at 12° S during April 7 – 8 (a), April 18 –25 (b), April 25 – May 3 (c), May 6 -12 (d), May 12 – 17 (e), May 17 – 26 (f) and June 24, 2017 (g).
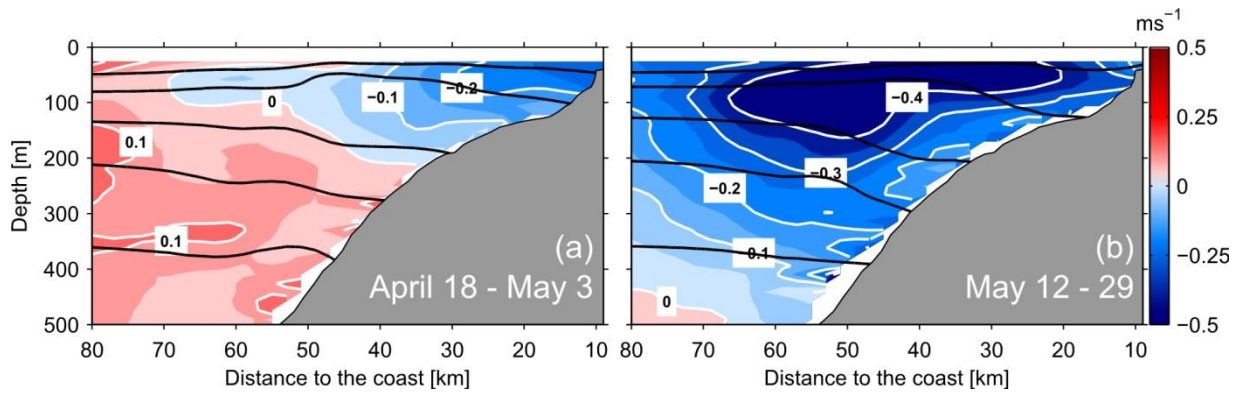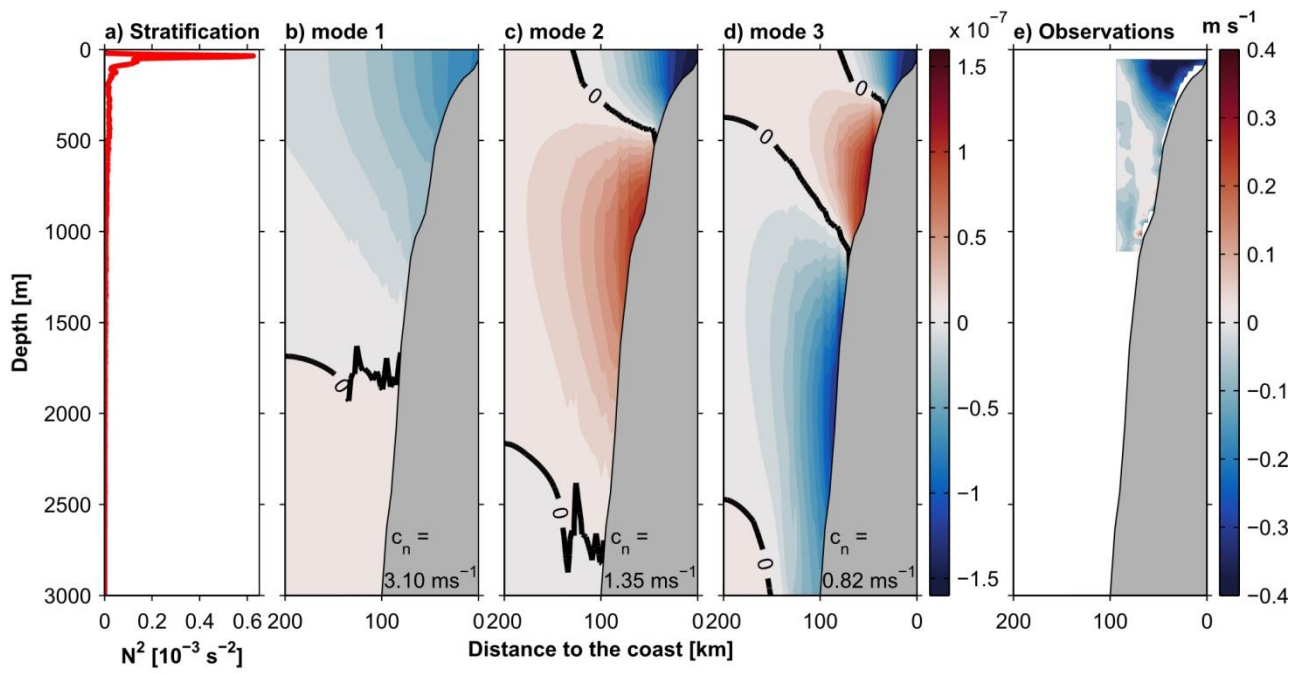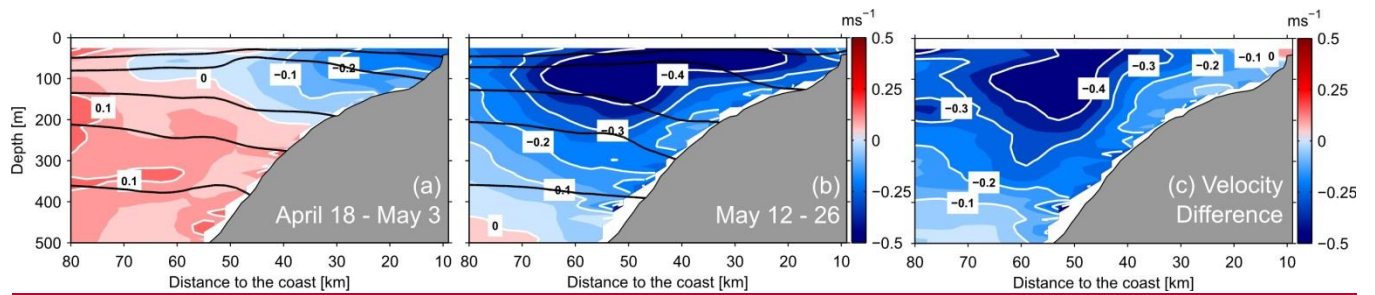
28

Figure 3: ~~Alongshore velocity at the 12 °S section off Peru from OS75 vmADCP, the~~ Black lines indicate the distribution of isopycnals (σθ) 25.6, 25.9, 26.2, 26.4, and 26.7 kg m-3 ~~isopycnals in black, during April 18 – May 3, 2017 (a), May 12 – 26, 2017 (b).~~.

Figure 3: Depth - distance distribution of averaged alongshore velocity at 12° S prior to (a, April 18 – May 3, 2017) and during (b, May 12 – 26, 2017) the PCUC intensification period. Panel c depicts the velocity difference between the two situations. Black lines indicate the distribution of isopycnals (σ_θ) 25.6, 25.9, 26.2, 26.4, and 26.7 kg m^{-3}.
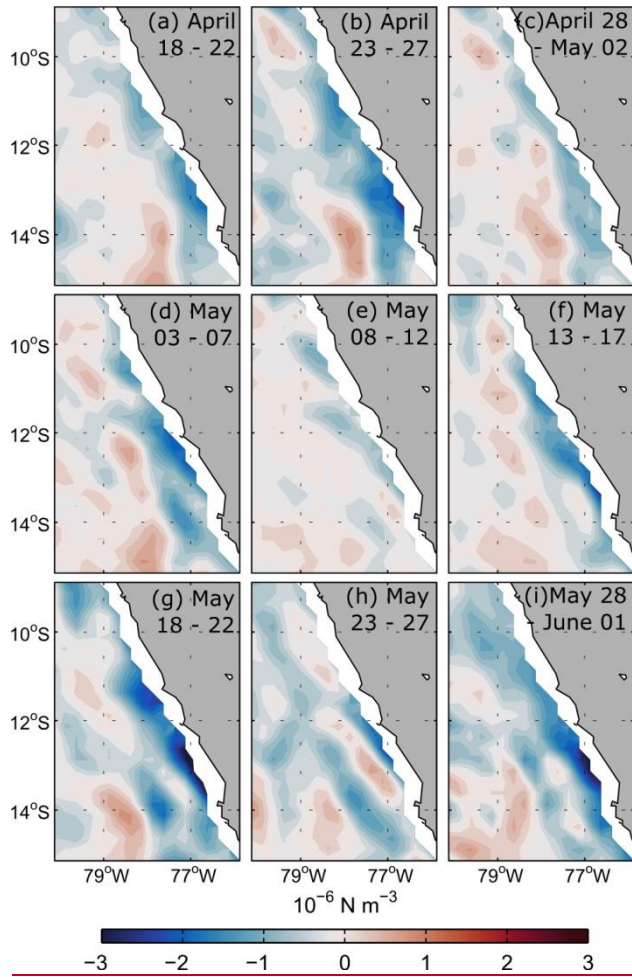
Figure 4: ~~Alongshore velocity structure (with arbitrary amplitude) and phase speed c_n (in the lower right corner) of the first~~ Five-day mean wind stress curl from ASCAT scatterometer winds off Peru during April 18 – 22 (a), April (23 – 27 (b), ~~second~~April 28 – May 02 (c), ~~and third mode~~May 03 – 07 (d), May 08 – 12 (e), May 13 – 17 (f), May 18 – 22 (g), May 23 – 27 (h) and May 28 – June 01, 2017 (i).
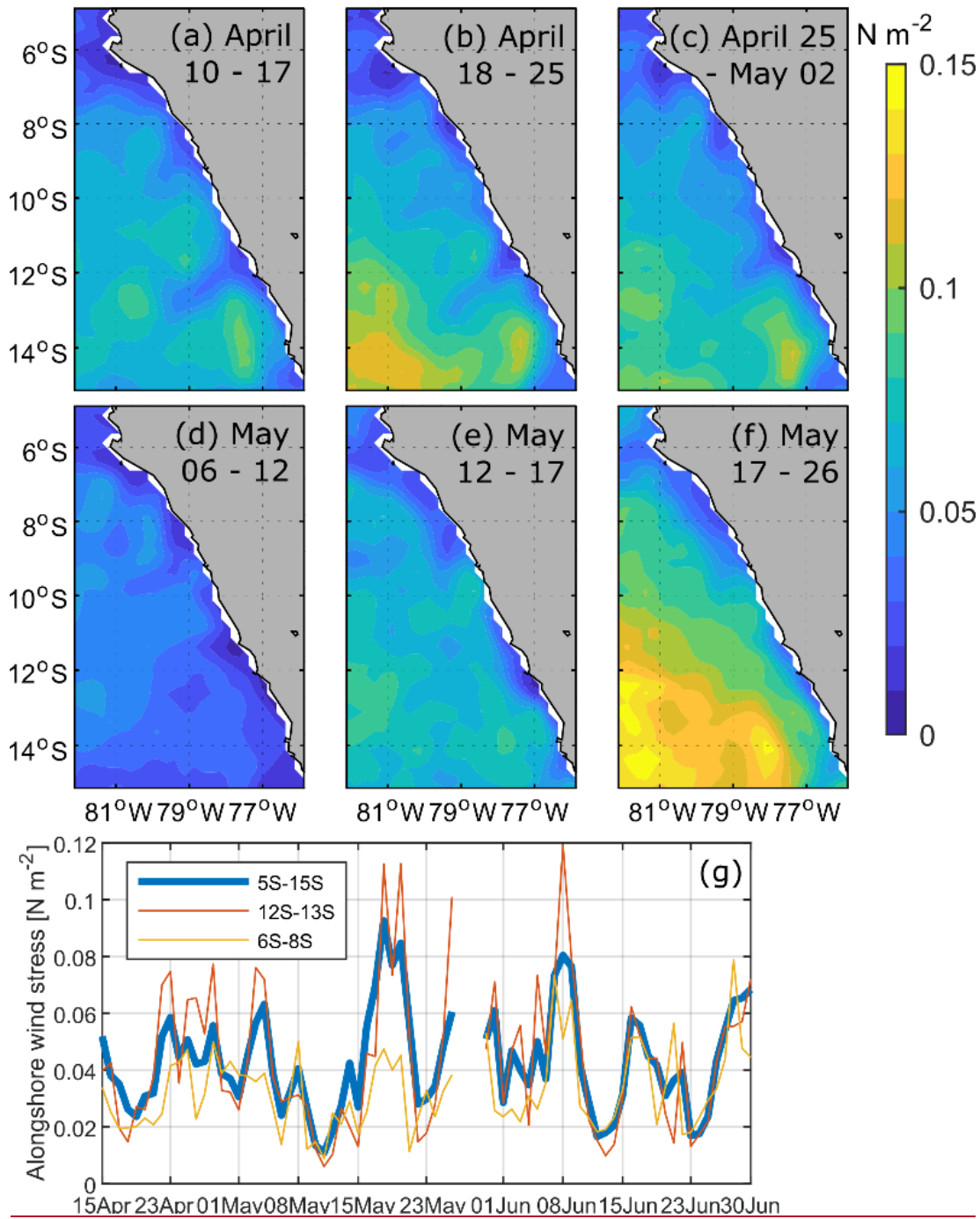
Figure 5: Weekly averages of alongshore wind stress from ASCAT scatterometer winds (upper two panel rows) for April 10 – 17 (a), April 18 -25 (b), April 25 – May 2 (c), May 06 – 12 (d), May 12 – 17 (e), May 17 – 26 (f). Lower panel (g) shows time series of alongshore wind stress averaged between 30 and 80 km from the coast for different bands of latitude.
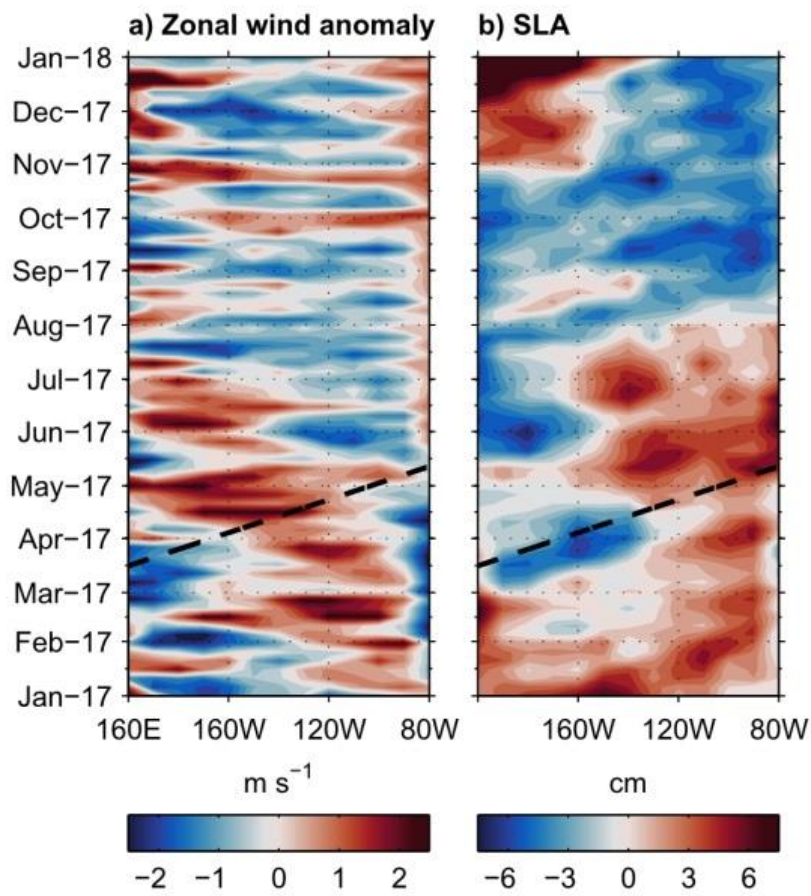
Figure 6: Hovmöller diagram of zonal wind anomaly (left panel) and SLA (right panel) along the central and eastern equatorial Pacific for the year 2017. The propagation of a first mode equatorial Kelvin wave is indicated by the dashed black line (phase speed 2.7 m s⁻¹; Yu and McPhaden, 1999).
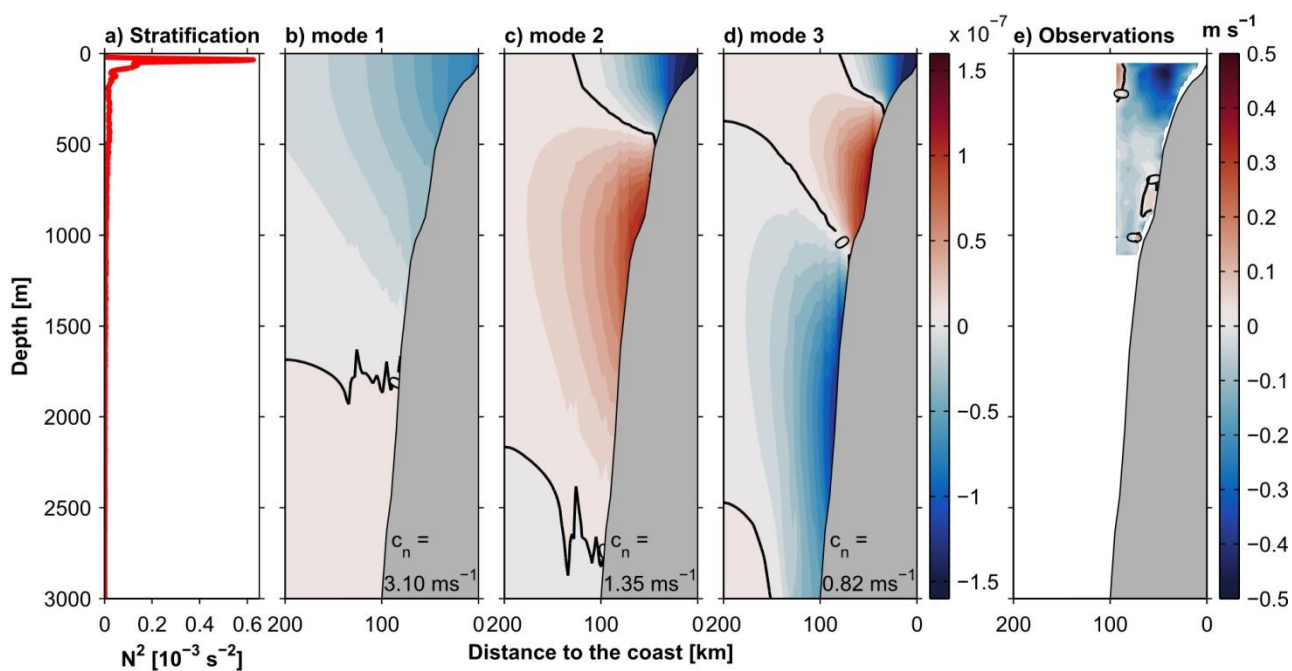
Figure 7: Profile of stratification (N²) (left panel) and cross-shore-depth structure of alongshore velocity (arbitrary amplitude) obtained for the first three CTW modes (panel b through d). Panel e) shows the difference of observed alongshore velocity ~~from OS38 vmADCP during May 12 – 29, 2017 (e)~~ between April 18 – May 03 and May 12 – 26, 2017. Note that the CTW phase speeds c_n are given in the lower right corner of the respective velocity structure panel.**
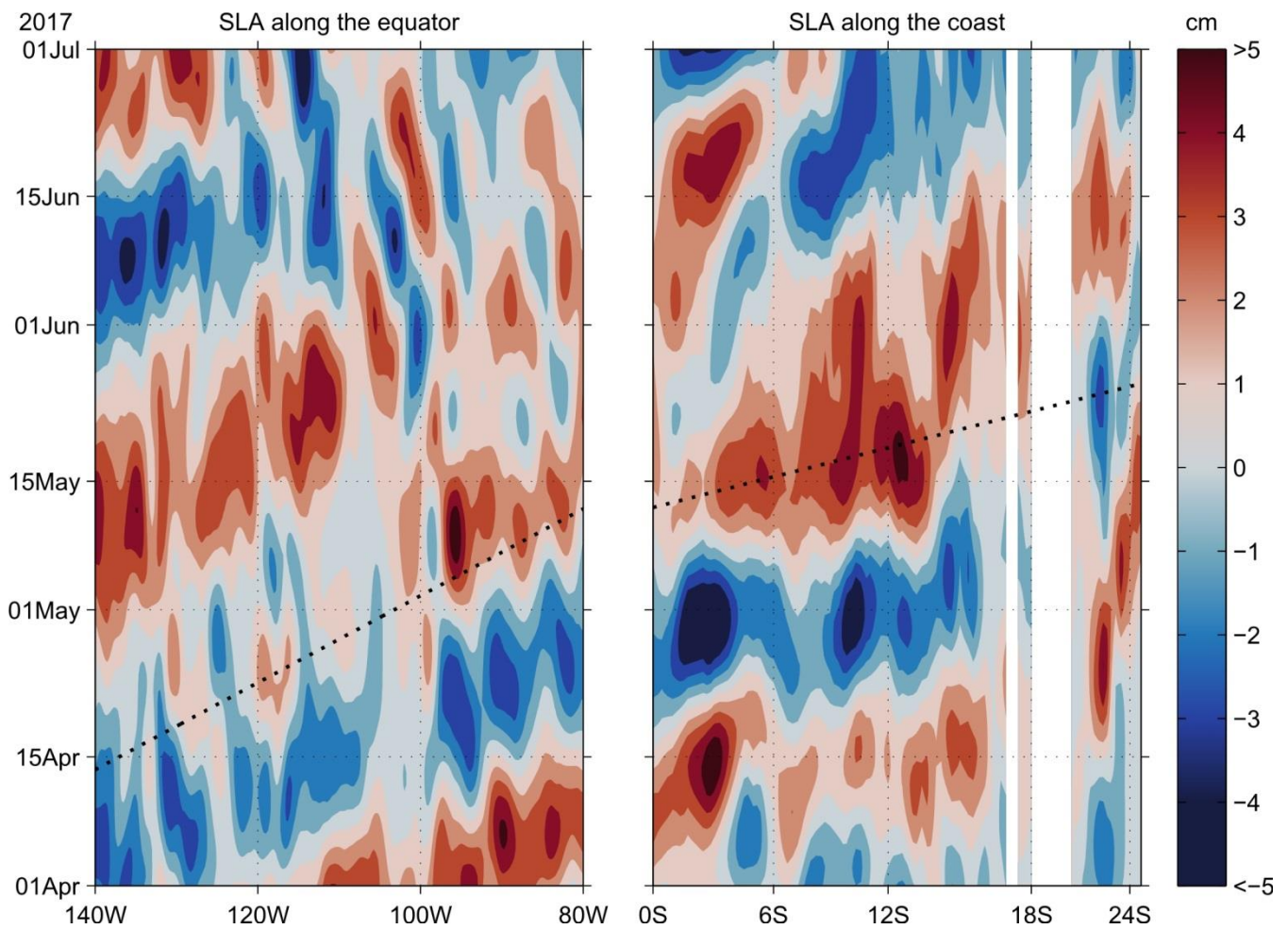
Figure 58: Bandpass filtered (20 – 90 days) sea level anomaly along the ~~equator (left)~~eastern equatorial Pacific averaged between 0.25°N and 0.25°S (left panel) and along the ~~South American~~western coast of South America (right panel) averaged over the two grid point closest to the coastline~~, the~~. The propagation of a first mode equatorial Kelvin wave and CTW are shown as dotted black lines, phase speed of the equatorial wave is 2.~~7~~27 m s^{-1} ~~after (~~Yu and McPhaden~~(~~, 1999) and 3.~~10~~1 m s^{-1} for ~~the CTW after the wave solution obtained in our study,~~ CTWs (see ~~Figure 4.~~figure 7b).
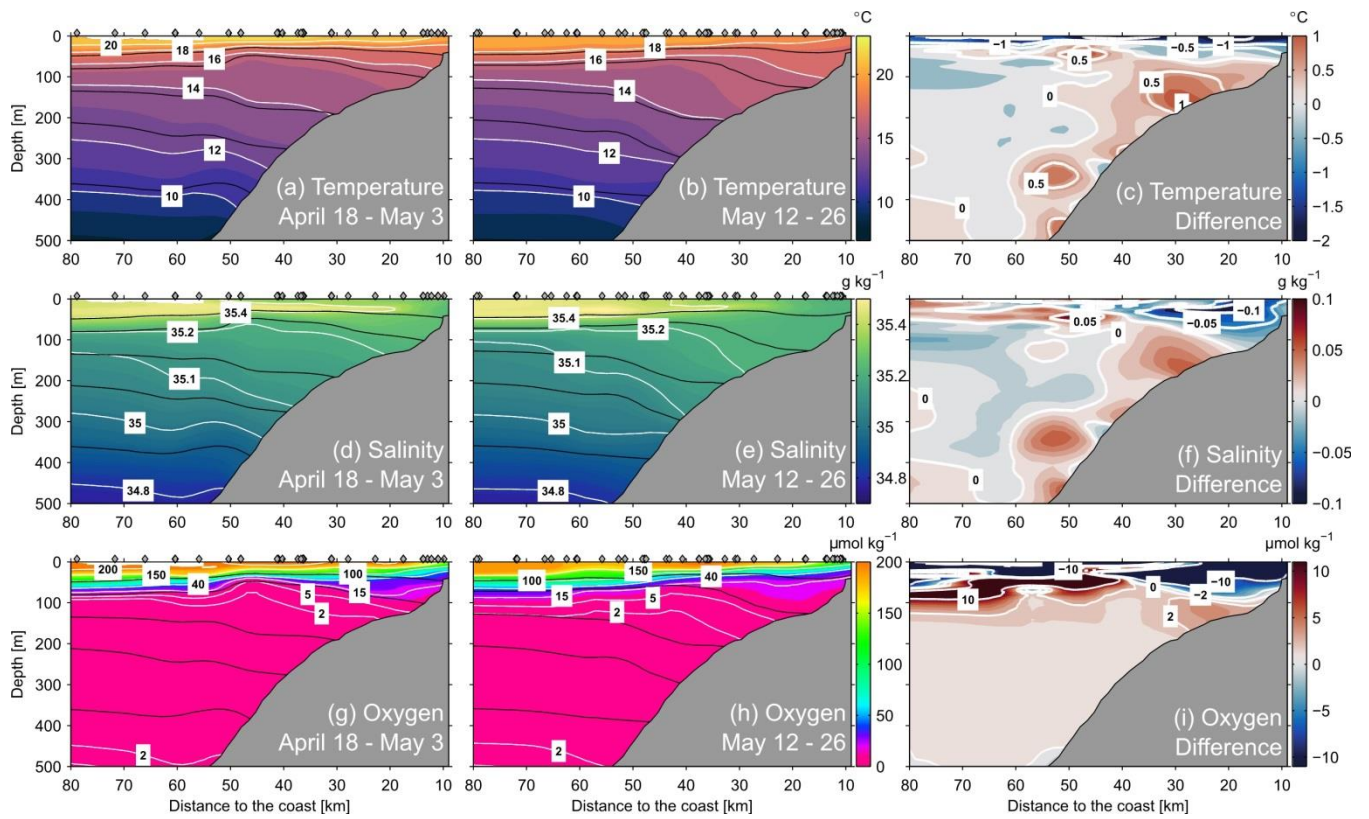
Figure 69: Conservative Temperature (upper panel row), absolute salinity (middle panel row), and oxygen (bottomlower panel row) along theat 12°S section off Peru during April 18 – May 3, 2017 (left panel column) and May 12 – 26, 2017 (middle panel column,.). The difference (right row), isolines of the shown parameter are shownrespective characteristic between the two periods is indicated in white, the 25.6, 25.9, 26.2, 26.4, and 26.7 kg m⁻³ the right panels. Black lines indicate the distribution of isopycnals are shown in black, grey (σθ) 25.6, 25.9, 26.2, 26.4, and 26.7 kg m⁻³. Grey diamonds mark the positions of profilesCTD stations.
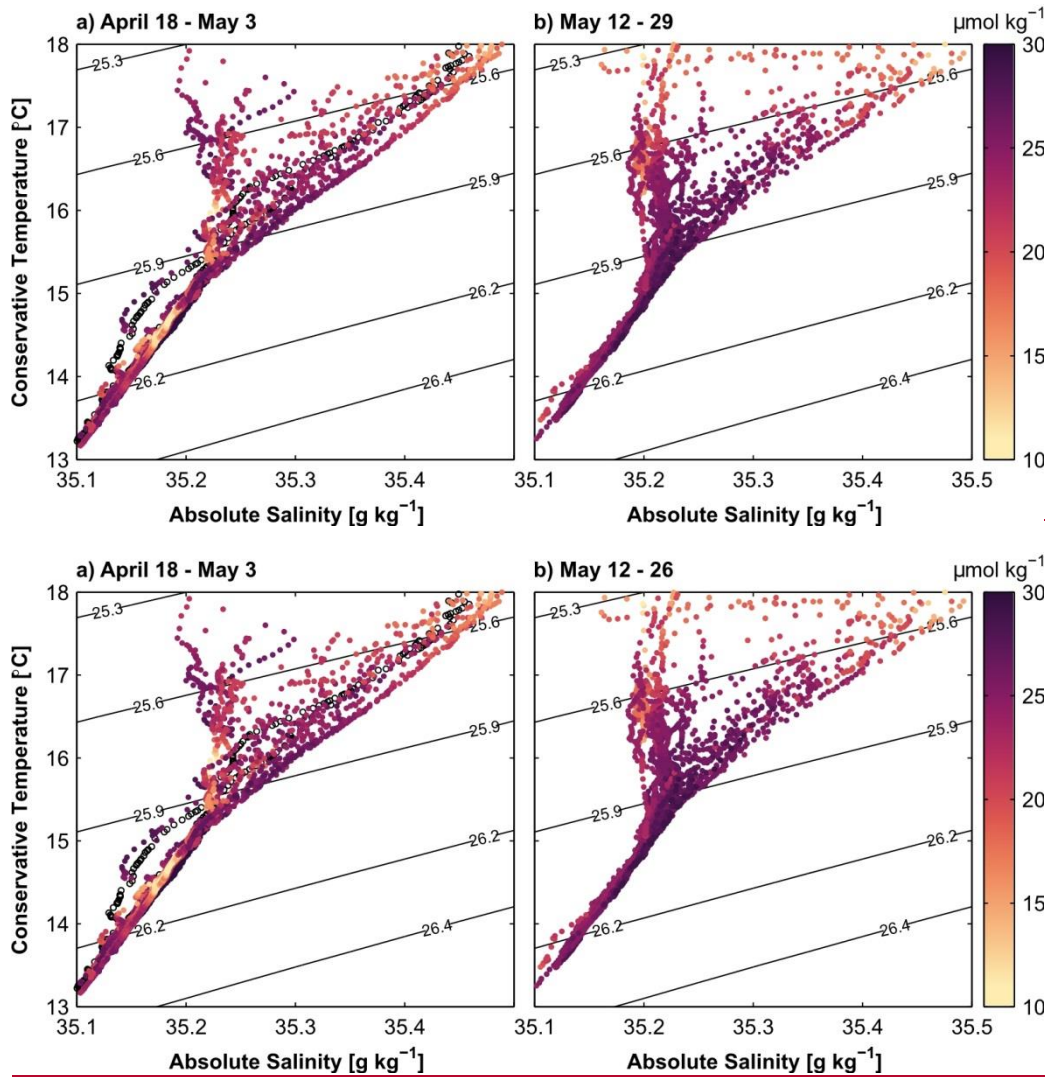
Figure 710: Conservative ~~Temperature – Absolute Salinity~~temperature – absolute salinity diagram between 50 and ~~300m~~300 m depth for CTD profiles between the 100 and ~~400m~~400 m isobaths during April 18 – May 3, 2017 (~~a~~left panel) and May 12 – 26, 2017 (~~b), contour lines show potential density anomalies corresponding to temperature and salinity on the axes, SUNA~~right panel). Colour code depicts nitrate concentrations ~~are shown as colour, empty circles are shown for profiles without SUNA data.~~ Black contours indicate isopycnals (σ_θ) in kg m^{-3}.
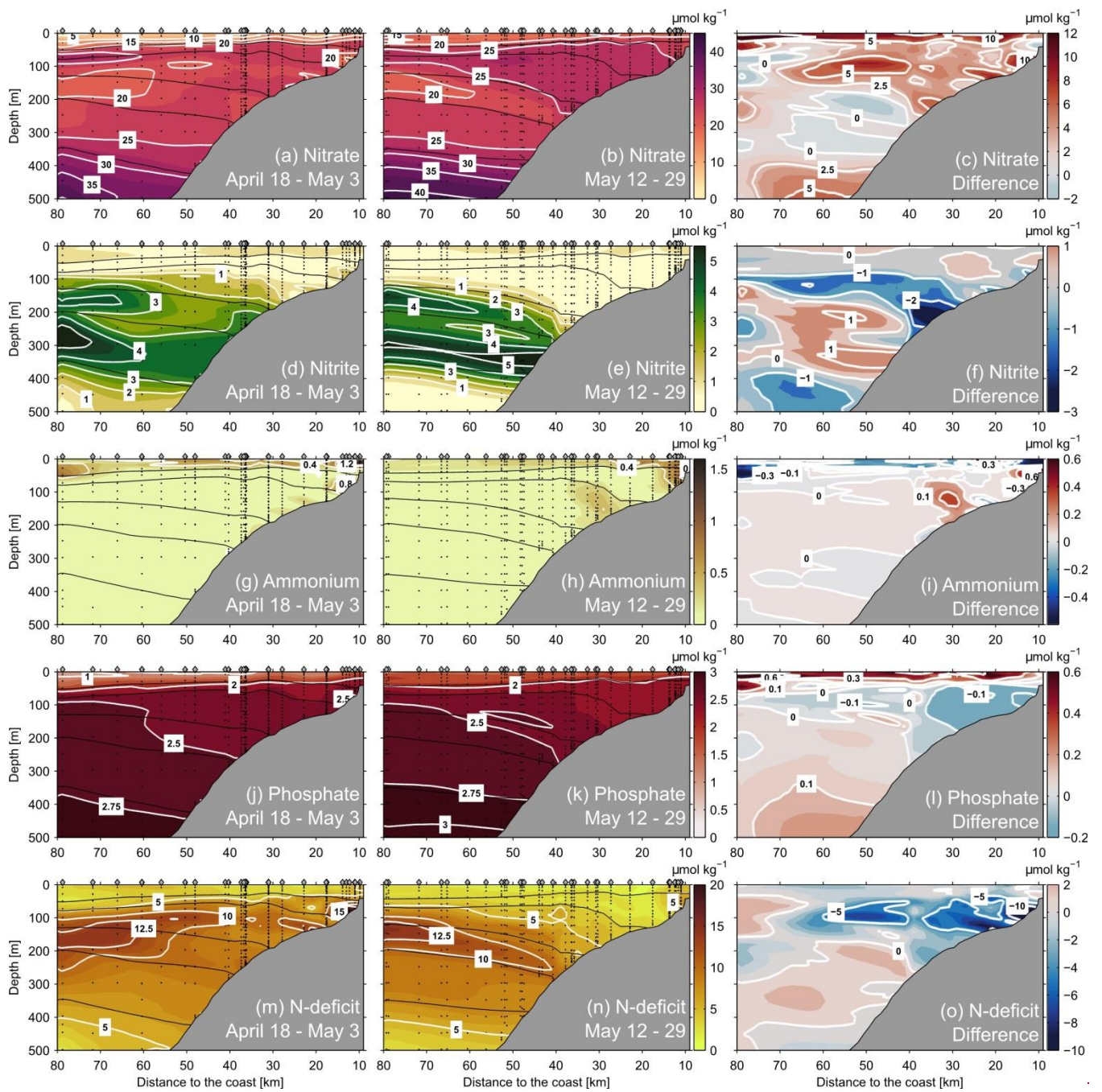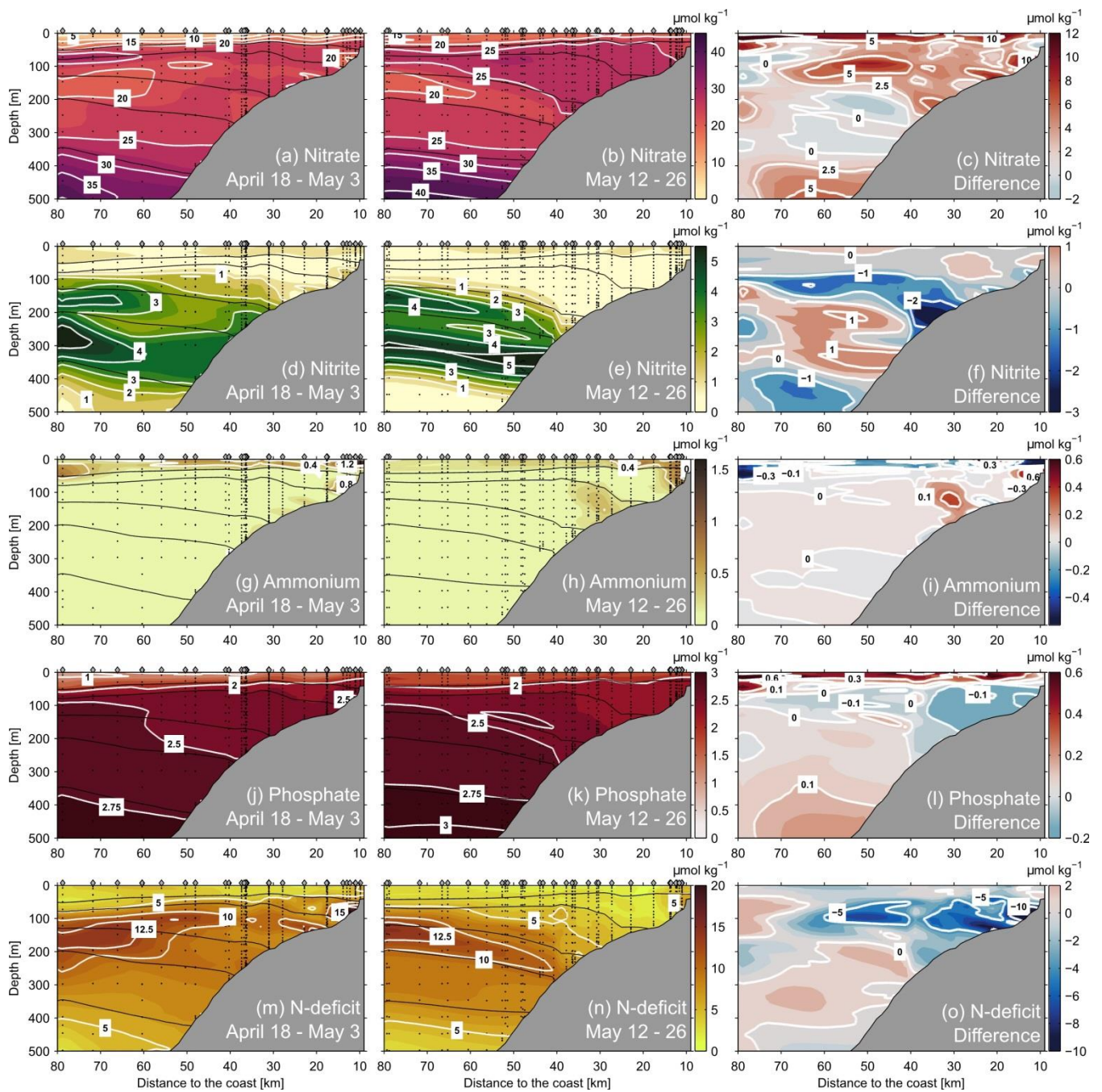
Figure ~~8~~11: Nitrate (~~first row~~upper panels), nitrite (~~second~~2nd panel row), ammonium (~~third~~3rd panel row), phosphate (~~fourth~~4th panel row) concentrations, and nitrogen deficit (~~fifth~~bottom panel row) at ~~the~~ 12°S ~~section off Peru~~ S during April 18 – May 3, 2017 (left ~~column~~panels) and May 12 – May 26, 2017 (middle ~~column),~~panels). Concentration difference (~~right row), isolines of the shown parameter~~of the respective parameters between the two time periods are shown ~~in white,~~the left panels. Black lines indicate the distribution of isopycnals (σθ) the 25.6, 25.9, 26.2, 26.4, and 26.7 kg m-3 ~~isopycnals are shown in black, grey.~~ Grey diamonds mark the positions of ~~profiles,~~CTD stations while black circles mark the position of bottle samples in the water column.

39